The interacting-boson model. Physical basis and applications

R. V. Jolos

Joint Institute for Nuclear Research, Dubna

I. Kh. Lemberg

Physicotechnical Institute, USSR Academy of Sciences, Leningrad

V. M. Mikhaĭlov

Leningrad State University

Fiz. Elem. Chastits At. Yadra **16**, 280–348 (March–April 1985)

The basis of the interacting-boson model and of the various modifications of it is reviewed together with its application to the description of the energy-level spectra and probabilities of electromagnetic transitions in even–even nuclei.

INTRODUCTION

In recent years, investigations of low-lying nuclear states have been interpreted more and more frequently by means of a phenomenological model proposed about ten years ago: the interacting boson model (IBM). This model combines Bohr and Mottelson's collective model with the assumption that the low-lying states of even–even nuclei are basically formed by a low-frequency quadrupole mode.

The appearance of quadrupole excitation quanta near magic nuclei, the gradual decrease in their energy and growth in their number, which leads to stable quadrupole deformations, and the subsequent return to the vibrational picture as the next closed shell is approached are described in the IBM by means of boson Hamiltonians, which contain not only the single-boson energy but also terms representing a pair interaction between the bosons, from which the name of the model derives. The microscopic prototype of the IBM bosons is provided by fermion pairing operators. In this sense, the IBM can be regarded as a phenomenological variant of the theory of boson expansions, the basic ideas of which were formulated before the appearance of the IBM. The development and application over a decade of the model have shown that the idea of boson mappings has been rather successfully implemented in the IBM, since the relative simplicity of both the original physical concept and the mathematical formalism of the model has enabled it to become one of the most widely used tools for studying the collective properties of low-lying states.

The popularity of the model in its two variants (IBM-I operates with bosons of just one species; IBM-II, with proton and neutron bosons separately) is to a large degree explained by two factors: first, the possibility of describing on a unified basis the significant changes that take place in the structure of the collective states of nuclei containing different numbers of nucleons, this being achieved by a smooth variation of the model parameters, and, second, the simplicity of application. The conclusions of the IBM and the Bohr-Mottelson collective model are to a large degree the same, and various studies have been devoted to the basis of the transition from the one to the other. However, the comparative simplicity of the algebraic methods employed in the IBM compared with the solution of differential equations in the Bohr-Mottelson model has made it possible to use the former for calculations for many nuclei in a wide range of A and to demonstrate the possibilities of the phenomenological approach for the description of collective states.

At the same time, calculations made have revealed some examples of disagreement with experimental results. In some cases, this is due to the basic limitations of the model. It considers only bosons with angular momenta 0 and 2. But as the spin of the excited states increases, bosons with $L = 4$, the so-called g bosons, must make a more and more important contribution to the structure of the states.

At sufficiently high excitation energies, one can expect the excitation of core nucleons. This leads to a change in the effective number of bosons (n_{eff}) compared with the number (n) usually considered, which is equal to half the number of valence nucleons or holes. Allowance for this effect on the basis of mixing of nuclear configurations with different numbers of bosons (n and n_{eff}) made it possible to explain features in the structure of a number of nuclei.

The IBM predicts a cutoff of the bands at $J = 2n$. This has not been observed experimentally. The excitation of core nucleons, and also allowance for g bosons, leads to values of n_{eff} greater than n, and thus makes the problem much less acute.

The properties of the purely collective states are distorted by their interaction with two-quasiparticle states, which appear in the energy spectrum at excitation energies $\geqslant 2\Delta$, where Δ is the gap energy. One of the possible ways to take into account this effect, like some other effects of interaction with noncollective states, is to introduce additional weakly collectivized bosons (s' and d').

It is hardly possible that all the observed discrepancies are due solely to the initial limitations of the IBM. Some of them may be due to a certain arbitrariness in the choice of the system of parameters of the IBM Hamiltonian by means of the optimization procedure. Cases have been known in which a choice of parameters that reproduce well the state energies or $B(E2)$ values leads to incorrect values and even opposite signs of the quadrupole moment of 2_1^+ states. It is not possible in all cases to reproduce the values of the transfer cross sections in the framework of the IBM.

Extensive testing of the conclusions of the IBM, using the results of investigations of various physical phenomena

 0090-4759/85/020121-32$04.40

such as reactions with the formation of a compound nucleus and direct transfer reactions, and measurements of quantities such as the energies of excited states, their lifetimes, and quadrupole and magnetic moments make it possible to determine more accurately the limits of applicability of this model and to give a sounder justification for the choice of its parameters.

An interesting feature of the model is also its clear algebraic structure, the dynamical symmetry group of which is SU(6). The possibility of finding analytic solutions in the cases when, for certain values of the parameters, the IBM Hamiltonian reduces to the Casimir operators of the SU(6) subalgebras establishes an affinity between the IBM and other nuclear theories that employ algebraic methods.

Since the inception of the IBM, there have been attempts to calculate the parameters of the model at the microscopic level. However, in this review we shall limit ourselves to a qualitative consideration of this problem, concentrating our main attention on the phenomenological aspects of the model. The first three sections are devoted to questions related to the basis of the model and its algebraic structure. In the following sections, we give examples of application of the model and consider some of its modifications.

1. IBM-I HAMILTONIAN

The solution of any problem in nuclear physics involves the separation of the dynamical variables that play the decisive part in some particular phenomenon. This applies to problems in both nuclear spectroscopy and nuclear reactions. It is necessary to separate explicitly in the Hamiltonian of the system considered the dependence on the most important dynamical variables, averaging over all the remaining degrees of freedom.

In the case of weakly excited nuclear states, the dynamical variables of quadrupole type are the most important. In the phenomenological collective nuclear model, such variables are represented by the components of the quadrupole deformation tensor. In the microscopic approach, the structure of the collective mode depends on the specific properties of the nucleus—the scheme of the single-particle levels, the single-particle wave functions, and the forces of the pair correlations and the quadrupole interaction. The structure is determined by solving the dynamical equations of the Tamm-Dancoff or random-phase approximations or modifications of them that take into account nonlinear corrections.

For example, in the Tamm-Dancoff approximation, the operator that generates the lowest quadrupole (2^+) excitation has the structure

$$A_\mu^+ = \frac{1}{\sqrt{2}} \sum_{jj'} \psi_{jj'} (\alpha_j^+ \alpha_{j'}^+)_\mu^{(2)}, \tag{1}$$

$$\sum_{jj'} \psi_{jj'}^2 = 1, \quad \psi_{jj'} \sim \langle j \| r^2 Y_2 \| j' \rangle (E_j + E_{j'} - \varepsilon)^{-1}.$$

Here, α_j^+ is the operator of creation of a quasiparticle in the state with angular momentum j [the other quantum numbers are not indicated explicitly in (1)], E_j is the single-quasiparticle energy, ε is the energy of the collective quadrupole excitation, and

$$(\alpha_j^+ \alpha_{j'}^+)_\mu^{(2)} = \sum_{m, m'} C_{jmj'm'}^{2\mu} \alpha_{jm}^+ \alpha_{j'm'}^+. \tag{1a}$$

The summation in (1) is over the states of the proton and neutron quasiparticles.

If $|0\rangle$ is the ground-state vector of the nucleus, then $A_\lambda^+ |0\rangle$ is the vector of the first 2^+ (2_1^+) state. However, such a description of the lowest 2^+ state is satisfactory only for a very restricted number of nuclei. At the same time, it is well known that the quadrupole branch of excitations is well separated from the other degrees of freedom in many even–even nuclei—spherical, transitional, and deformed. The experiments give good grounds for describing the properties of the low-lying states of these nuclei on the basis of a Hamiltonian containing only collective quadrupole variables.

The Hamiltonian of a nucleus with a two-particle residual interaction, expressed in terms of quasiparticle creation and annihilation operators, has the structure

$$H = \sum_{jm} E_j \alpha_{jm}^+ \alpha_{jm} + \sum_{(j_i)} \{V_{j_1 j_2 j_3 j_4}^{(1)} (\alpha_{j_1}^+ \alpha_{j_2}^+ \alpha_{j_3}^+ \alpha_{j_4}^+ + \text{h.c.}) + V_{j_1 j_2 j_3 j_4}^{(2)} (\alpha_{j_1}^+ \alpha_{j_2}^+ \alpha_{j_3}^+ \alpha_{j_4} + \text{h.c.}) + V_{j_1 j_2 j_3 j_4}^{(3)} \alpha_{j_1}^+ \alpha_{j_2}^+ \alpha_{j_3} \alpha_{j_4}\}. \tag{2}$$

Using now the operators A_λ^+ as the operators of quadrupole phonons, we construct a basis of many-phonon states

$$A_\mu^+ |0\rangle, \ \frac{1}{\sqrt{2}} (A^+ A^+)_M^{(L)} |0\rangle \ldots \tag{3}$$

and we diagonalize the Hamiltonian H in this basis. [In (3) and in what follows, $(\ldots)_M^{(L)}$ means that the operators in the brackets are coupled to give angular momentum L and projection M.]

We begin with the construction of the basis. The coefficients $\psi_{jj'}$ are defined in such a way that the state $A_\lambda^+ |0\rangle$ is normalized to unity. All the remaining states, being constructed as if from ideal phonon operators, will have a norm that is less than unity and decreases with increasing number of quasiparticle operators (the operators A_λ^+) used in the construction of the state vector. This result is a consequence of the Pauli principle, which is readily seen by calculating, for example, the norm of the state

$$\frac{1}{\sqrt{2}} (A^+ A^+)_M^{(L)} |0\rangle. \tag{4}$$

If the operators A_λ^+ were identical to ideal boson quadrupole operators d_λ^+ satisfying the commutation relations

$$[d_\mu, \ d_{\mu'}^+] = \delta_{\mu, \mu'},$$

then the norm of the vector (4) would be unity. But in our case

$$\frac{1}{2} \langle 0 | (AA)_M^{(L)} (A^+ A^+)_M^L | 0 \rangle = 1 - 50 \sum_{j_1 j_2 j_3 j_4} \psi_{j_1 j_3} \psi_{j_1 j_2} \times \psi_{j_3 j_4} \psi_{j_2 j_4} \begin{Bmatrix} j_1 & j_3 & 2 \\ j_2 & j_4 & 2 \\ 2 & 2 & L \end{Bmatrix}.$$

If the operator A_λ^+ is formed from quasiparticles of only one subshell with spin $j \gg 1$, then (for $L = M = 0$)

$$\frac{1}{2} \langle 0 | (AA)^{(0)} (A^+ A^+)^{(0)} | 0 \rangle \simeq 1 - \frac{1}{\frac{1}{5}\left(j + \frac{1}{2}\right)}.$$

The higher the degeneracy of the state of the subshell, i.e., the greater the number of components in the phonon operator, the nearer is the norm of the state (3) to unity. We introduce the notation

$$\frac{1}{2}\langle 0 \mid (AA)^{(L)}_M\,(A^+A^+)^{(L)}_M \mid 0\rangle = 1-(\Omega_L)^{-1}.$$

Specific calculations show that Ω_L depends on the spin of the state but that this dependence is weaker, the heavier the nucleus that is considered. With increasing A and with increasing distance from closed shells, the value of Ω_L increases. Microscopic calculations of Ω_L were made in Refs. 1 and 2. In order of magnitude, Ω_L is equal to the number of valence pairs of particles or holes.

The calculation of the norm of a state containing more than two operators A_λ^+ is much more complicated, but it is possible to find approximate recursion relations[1,2] for the norms of the states, and these give the result

$$\langle 0 \mid \underbrace{(A\ldots A)}_{n}{}^{(L)}_M\ \underbrace{(A^+\ldots A^+)}_{n}{}^{(L)}_M \mid 0\rangle = \left(1-\frac{1}{\Omega}\right)\left(1-\frac{2}{\Omega}\right)\ldots\left(1-\frac{n-1}{\Omega}\right). \tag{5}$$

The structure of the state vector in (5) is such that if A_λ^+ is replaced by d_λ^+, then 1 will appear on the right-hand side in (5). Using (5), we can readily find the boson image of the operator A_λ^+:

$$A_\mu^+ \to d_\mu^+\sqrt{1-\frac{\hat n_d}{\Omega}}\,, \qquad \hat n_d = \sum_\mu d_\mu^+ d_\mu. \tag{6}$$

One can now verify that substitution of (6) in the left-hand side of (5) gives the result given on the right. It follows from (5) and (6) that the parameter Ω, taken to be integral, is the maximal number of d bosons that can be present in the wave function. It can also be seen from (5) and (6) that the introduction of the operator $\sqrt{1-\hat n_d/\Omega}$ takes into account the Pauli principle approximately.

We turn to the quasiparticle nuclear Hamiltonian (2). Using (6), we find the boson images of the operators $\alpha_j^+\alpha_{j'}^+$:

$$\alpha^+_{jm}\alpha^+_{j'm'} = \sum_{L\mu} C^{L\mu}_{jmj'm'}\,(\alpha^+_j\alpha^+_{j'})^{(L)}_\mu \simeq C^{2\mu}_{jmj'm'}\,(\alpha^+_j\alpha^+_{j'})^{(2)}_\mu$$

$$\simeq \sqrt{2}\,\psi_{jj'}C^{2\mu}_{jmj'm'}A^+_\mu \to \sqrt{2}\,\psi_{jj'}C^{2\mu}_{jmj'm'}d^+_\mu\sqrt{1-\hat n_d/\Omega}\,. \tag{7}$$

In the same approximation, we also find the boson image of the operator $\alpha_{j1}^+ a_{j2}$. Since this operator does not change the number of quasiparticles, its boson image is proportional to $d_\lambda^+ d_\nu$:

$$\alpha^+_{j_1m_1}\alpha_{j_2m_2} \simeq 2\sum_{jm\mu\nu}\psi_{j_1j}\psi_{j_2j}C^{2\mu}_{j_1m_1jm}C^{2\nu}_{j_2m_2jm}d^+_\mu d_\nu. \tag{8}$$

When the fermion pairing operators are mapped to the boson operators, we obtain an infinite series in bosons of different types (see, for example, Ref. 3). In (7) and (8), we have retained only the d-boson operators on the strength of the basic assumption that the subspace generated by the fermion operators A_λ (1) and by the d bosons corresponding to them is sufficiently closed, this being equivalent to the assumption that the terms of the Hamiltonian that couple this subspace to the states determined by the other degrees of freedom are small.

Substituting (7) and (8) in the Hamiltonian (2), we obtain the boson Hamiltonian[4-6]

$$\begin{aligned} H = {} & \varepsilon\hat n_d + \varkappa_1\sum_\mu\left(d^+_\mu\sqrt{\Omega-\hat n_d}\,\tilde d^+_\mu\sqrt{\Omega-\hat n_d} + \text{h.c.}\right) \\ & + \varkappa_2\sum_\mu\left[d^+_\mu\sqrt{\Omega-\hat n_d}\,(d^+d)^{(2)}_\mu + \text{h.c.}\right] \\ & + \frac{1}{2}\sum_{L=0,\,2,\,4;\,\mu} c_L\,(d^+d^+)^{(L)}_\mu\,(\tilde d\tilde d)^{(L)}_\mu \end{aligned} \tag{9}$$

(the bar above an index means time conjugation). One can find similarly the boson image of the electric quadrupole transition operator $\hat T_\mu(E2)$. The operator $\hat T_\mu(E2)$, expressed in terms of quasiparticles, contains pairing operators of the form $(\alpha_{j_1}^+\alpha_{j_2})^{(2)}_\mu$ and $(\alpha_j^+\alpha_{\bar j}^+ + \alpha_{\bar j}\alpha_j)^{(2)}_\mu$, so that, again using (7) and (8), we obtain

$$\hat T_\mu(E2) = q_0\left(d^+_\mu\sqrt{\Omega-\hat n_d} + \sqrt{\Omega-\hat n_d}\,\tilde d_\mu\right) + q_1\,(d^+\tilde d)^{(2)}_\mu. \tag{10}$$

The Hamiltonian (9) and the $E2$-transition operator (10) are combinations of terms linear and quadratic in the operators

$$d^+_\mu\sqrt{\Omega-\hat n_d}, \quad \sqrt{\Omega-\hat n_d}\,d_\mu, \quad d^+_\mu d_\nu, \tag{11}$$

which form the SU(6) algebra, as can be readily seen by calculating their commutators.

The construction of the collective Hamiltonian from the generators of the group SU(6) has been made possible because the factor that takes into account approximately the Pauli principle has the form of the square root $\sqrt{\Omega-\hat n_d}$ and depends only on the number of bosons. This circumstance, and also the fact that $\sqrt{\Omega-n_d}$ vanishes when the number of bosons becomes equal to Ω, and does not decrease smoothly to zero as the number of bosons is gradually increased, are consequences of the approximations that have been made.

We now consider how the collective Hamiltonian is changed by a more accurate calculation of the normalization coefficients (4) with allowance for their dependence not only on the number of bosons (n), but also on the seniority (v) and the spin of the state (L). The number v is determined as the number of bosons among which there are no pairs with vanishing angular momentum:

$$N(n,\ v,\ L) = \langle 0 \mid (A\ldots A)^{(Lnv)}_M\,(A^+\ldots A^+)^{(Lnv)}_M \mid 0\rangle. \tag{12}$$

The calculations show that even if the spin dependence is ignored the following result is obtained[7]:

$$\left.\begin{aligned} \frac{N(n+1,\ v+1)}{N(n,\ v)} &= \left(1-\frac{n+v}{2\varkappa}\right)\left(1-\frac{n}{\Omega}\right); \\ \frac{N(n+1,\ v-1)}{N(n,\ v)} &= \left(1-\frac{n-v-3}{2\varkappa}\right)\left(1-\frac{n}{\Omega}\right). \end{aligned}\right\} \tag{13}$$

One can also take into account the dependence of N on the spin of the state by obtaining recursion relations,[1,7] which give the exact values for the normalization coefficients for $n=2$ and 3 and approximate values for large n. Apart from the fact that $N(n, v, L)$ depend on n, v, and L, they do not vanish at some maximal value of n but decrease smoothly with increasing n.

We now introduce the Hermitian operator $\hat{N}(d^+, d)$, which is diagonal in a basis formed from vectors with a fixed number of bosons, and we determine $\hat{N}$ in such a way that its diagonal matrix elements are equal to those of $N(n, v, L)$. In this case,

$$A_\mu^+ \to \hat{N}^{1/2} d_\mu^+ \hat{N}^{-1/2}. \tag{14}$$

Substitution of (14) in the expression (12) for N leads to an identity. The collective Hamiltonian can now be constructed for arbitrary values of the normalization coefficients:

$$H = \varepsilon \hat{n}_d + \kappa_1 \left[\hat{N}^{1/2} \left(\sum_\mu d_\mu^+ d_\mu^+ + \text{h.c.} \right) \hat{N}^{-1/2} \right] + \kappa_2 \hat{N}^{1/2} \left[\sum_\mu d_\mu^+ (d^+ d)_\mu^{(2)} + \text{h.c.} \right] \hat{N}^{-1/2} + \frac{1}{2} \sum_{L,\mu} c_L \hat{N}^{1/2} (d^+ d^+)_\mu^{(L)} (dd)_\mu^{(L)} \hat{N}^{-1/2}. \tag{15}$$

If it is assumed, as is done in (5), that N depends only on the number of bosons n, i.e.,

$$\frac{N(n+1)}{N(n)} = 1 - \frac{n}{\Omega}, \tag{16}$$

then the expressions (14) and (15) go over into (6) and (9), respectively.

The simplification used in (5) for the normalization coefficients has made it possible to express H (9) and $\hat{T}(E2)$ (10) in terms of the generators (11) of the group SU(6). The representation of the algebra by means of the boson operators (11) has become known as the Primakoff–Holstein representation.[8] The characteristic feature of this representation is the presence in the generators (11) of the parameter Ω, which determines the maximal number of bosons in the basis functions, which are constructed as superpositions of the states

$$|0), \ d^+|0), \ d^+d^+|0), \ \ldots, \underbrace{(d^+ \ldots d^+)}_{n}|0), \quad n \leqslant \Omega, \tag{17}$$

where $|0)$ is the boson vacuum.

The generators of the SU(6) algebra have a different boson representation—the Schwinger representation,[9] which uses the operators of creation and annihilation of the d bosons and of the additional scalar boson s:

$$d_\mu^+ s, \ s^+ d_\mu, \ d_\mu^+ d_\nu - \delta_{\mu,\nu} s^+ s. \tag{18}$$

Formally, the algebra of the operators (18) does not contain an indication of the number of bosons to which it corresponds, but states with a quite definite boson number, which we also call Ω, are its basis functions:

$$(s^+)^{\Omega - n} \underbrace{(d^+ \ldots d^+)}_{n}|0), \quad n \leqslant \Omega, \tag{19}$$

i.e., the total number of s and d bosons is Ω.

It was shown in Refs. 10 and 11 that the representations (11) and (18) go over into each other under a unitary transformation, i.e., these representations are equivalent. To construct the Hamiltonian and the $E2$-transition operator by means of (18), we perform in the operators (9) and (10) the substitutions

$$d_\mu^+ \sqrt{\Omega - \hat{n}_d} \to d_\mu^+ s; \quad \sqrt{\Omega - \hat{n}_d}\, d_\mu \to s^+ d_\mu; \quad d_\mu^+ d_\nu \to d_\mu^+ d_\nu, \tag{20}$$

as a result of which we obtain

$$H = \varepsilon \hat{n}_d + \kappa_1 \sum_\mu (d_\mu^+ d_\mu^+ ss + \text{h.c.}) + \kappa_2 \sum_\mu [d_\mu^+ (d^+ d)_\mu^{(2)} s + \text{h.c.}] + \frac{1}{2} \sum_{L=0,2,4;\mu} c_L (d^+ d^+)_\mu^{(L)} (dd)_\mu^{(L)}; \tag{21}$$

$$\hat{T}_\mu(E2) = q_0 (d_\mu^+ s + s^+ d_\mu^-) + q_1 (d^+ d)_\mu^{(2)} \equiv e^* [d_\mu^+ s + s^+ d_\mu^- + \chi_{E2} (d^+ d)_\mu^{(2)}]. \tag{22}$$

The question of the equivalence of the Hamiltonians (9) and (21) is considered in detail in Refs. 10–13.

A Hamiltonian composed of s and d bosons was proposed for the first time by Arima and Iachello[15] (from whom the standard name of the model also derives) as the most general scalar Hermitian operator containing not more than four boson operators:

$$H = \varepsilon_s \hat{n}_s + \varepsilon_d \hat{n}_d + \frac{1}{2} u_0 s^+ s^+ ss + u_2 \hat{n}_s \hat{n}_d + \frac{1}{\sqrt{2}} v_0 [(d^+ d^+)^0 ss + \text{h.c.}] + v_2 [(d^+ (d^+ d)^{(2)})_s^{(0)} + \text{h.c.}] + \frac{1}{2} \sum_{L=0,2,4} \tilde{c}_L + ((d^+ d^+)^{(L)} (dd)^{(L)})^{(0)}. \tag{23}$$

When allowance is made for the relation $\Omega = \hat{n}_s + \hat{n}_d (n_s = s^+ s)$ and the use of the commutation relations between the boson operators, the Hamiltonian (23) can be reduced to the form (21), so that the total number of independent constants in the IBM Hamiltonian is six ($\varepsilon, \varkappa_1, \varkappa_2, c_0, c_2, c_4$). In what follows, we shall refer to the Hamiltonian in the form (9) or (21) as the IBM-I Hamiltonian—the Hamiltonian of the model in its first variant, which does not take into account the differences between the proton and neutron bosons.

We have outlined above a method for constructing the collective Hamiltonian based on the use of the quasiparticle operators $A_\lambda^+(1)$, which act on the vacuum state $|0\rangle$. It is, however, well known that when quasiparticle operators are employed a certain inaccuracy arises because of nonconservation of the particle number. In principle, this inaccuracy can be eliminated by replacing the operators A_λ^+ by a superposition of particle-hole quadrupole operators, and the quasiparticle vacuum by a state that could, for example, be obtained by projection with respect to the particle number of Bardeen–Cooper–Schrieffer functions. However, in both quasiparticle theory and a theory with conservation of the particle number only quadrupole fermion operators are used to introduce the boson Hamiltonian, and no need arises for the introduction of a special scalar operator.

The Hamiltonian (9) (without s bosons) and the Hamiltonian (21) (containing s bosons) go over into each other under a unitary transformation, and they are therefore physically equivalent. Thus, it can be assumed that the introduction of the s boson in (21) and (22) is formal in nature, its introduction being a convenient way of replacing the operators $\sqrt{\Omega - \hat{n}_d}$. Note that the scalar boson was introduced for the first time in Refs. 5 and 14 precisely for this purpose. At the present time, various forms of the IBM-I

Hamiltonian are used in the literature; they differ in the ways used to couple the boson operators. All these forms go over into one another when certain relationships between the constants are satisfied. A list of the different forms of the IBM-I Hamiltonian and the relationships between the constants is given in Ref. 16. We give here one of the possible forms of the Hamiltonian (21), in which we explicitly separate the quadrupole-quadrupole interaction between the bosons:

$$\left.\begin{aligned} H &= \tilde{\varepsilon}\hat{n}_d + \kappa_1 \sum_{\mu} Q_{\mu}^{+} Q_{\mu} + \frac{1}{2} \sum_{L,\,M} c'_L \,(d^{+}d^{+})_{\mu}^{(L)} \,(dd)_{\mu}^{(L)}; \\ Q_{\mu} &= d_{\mu}^{+}s + s^{+}d_{\tilde{\mu}} + \chi\,(d^{+}d)_{\mu}^{(2)}; \quad \chi = \kappa_2/2\kappa_1; \end{aligned}\right\} \tag{24}$$

in (24), the parameters $\tilde{\varepsilon}$ and c'_L are linear functions of the parameters $\varepsilon, \kappa_1, \kappa_2$, and c_L of the Hamiltonian (21). If there is proportionality between the values of the proton and neutron matrix elements of the quadrupole operator, then in such a case one can expect the parameter in (24) to be close to the parameter χ_{E2} in the $E2$-transition operator in (22).

2. DESCRIPTION OF THE PROPERTIES OF SPHERICAL, TRANSITIONAL, AND DEFORMED NUCLEI ON THE BASIS OF THE IBM-I

The Hamiltonian (21) is not the only one that has been proposed for the description of the properties of the quadrupole excitations of even-even nuclei. We should recall the harmonic oscillator for spherical nuclei, the quasiparticle-phonon model for the description of the vibrational excitations of strongly deformed nuclei, Elliott's model for describing rotational bands, and, finally, the generalized Bohr-Mottelson model. The majority of these models could describe only a certain type of excitation of deformed nuclei. In principle, the Bohr-Mottelson Hamiltonian can describe the spectra of quadrupole excitations of all nuclei from the spherical to the deformed. However, the parametrization of the vibration energies for transitional nuclei is a difficult task and requires many parameters.

Experimentally, all possible excitation spectra are observed. Moreover, in a number of cases, tracing the change in the spectrum of states along the chain of isotopes of a given element, one can observe a smooth transition from spherical to deformed nuclei. The behavior of the nuclei in the transitional region is different for different regions of mass numbers. The question arises of whether it is possible to describe this picture by means of the Hamiltonian (21).

It is not difficult to see that spherical nuclei can be described by the Hamiltonian (21). Setting $\kappa_1 = \kappa_2 = 0$, we obtain from (21) a Hamiltonian whose eigenstates are states with a fixed number of quadrupole phonons. For $c_L = 0$, the spectrum of the excited states is equidistant. For small but nonvanishing c_L, weak deviations from equidistance are observed. In this case, an exact result can be obtained analytically [SU(5), the IBM limit], since the Hamiltonian (21) can be expressed in terms of the Casimir operators of SU(6) subgroups[1,6,15]:

$$SU\,(6) \supset SU\,(5) \supset O\,(5) \supset O\,(3), \tag{25}$$

and its eigenvalue in terms of the quantum numbers of the subgroups in the chain (25):

$$E = a_1 n + a_2 n^2 + a_3 v\,(v+3) + a_4 I\,(I+1), \tag{25a}$$

where n is the number of quadrupole bosons [SU(5)], v is the seniority [O(5)], and I is the angular momentum of the state [O(3)]. The parameters a_i in (25a) are related linearly to the parameters of the Hamiltonian (21).

Since the quadrupole component is dominant in the residual forces, the vanishing of the coefficient κ_2 in the Hamiltonian must mean that the coefficient χ_{E2} in (22) also vanishes. Then for the probabilities of $E2$ transitions we obtain, apart from corrections of order Ω^{-1}, the same relations as in the model of harmonic quadrupole vibrations.

The eigenvalue spectrum of the Hamiltonian (21) is shown in Fig. 1. It can be seen from the figure that with increasing κ_2 the spectrum of states changes from being equidistant to having a rotational type. The nature of the transition depends on the value of κ_1. At small κ_1, a sharp lowering of the 0_2^+ state is observed. With increasing κ_1, the lowering decreases, and at sufficiently large κ_1 there is a smooth transition from a vibrational to a rotational spectrum with the formation of quasirotational bands in the transitional region. Transitional nuclei with low-lying 0_2^+ states are known experimentally (see Sec. 7 below).

The nature of the dependence of the energy spectrum on κ_2 indicates that this parameter plays in the IBM the same role as the parameter associated with the terms in the potential energy of the shape vibrations of the nucleus that depend on γ [the coefficient of $V(\beta^2)\beta^3\cos 3\gamma$]. This conclusion is also confirmed by microscopic calculations of the coefficient κ_2, whose value is determined by the asymmetry in the distribution of the interaction matrix elements with respect to the Fermi surface.

As we have already noted, nonvanishing of the coefficient κ_2 also entails nonvanishing of the coefficient χ_{E2} in the expression for the operator of the quadrupole transitions in (22). For large values of the coefficients κ_1 and κ_2 in the Hamiltonian, results characteristic of strongly deformed nuclei are obtained for the $E2$-transition probabilities and static quadrupole moments.

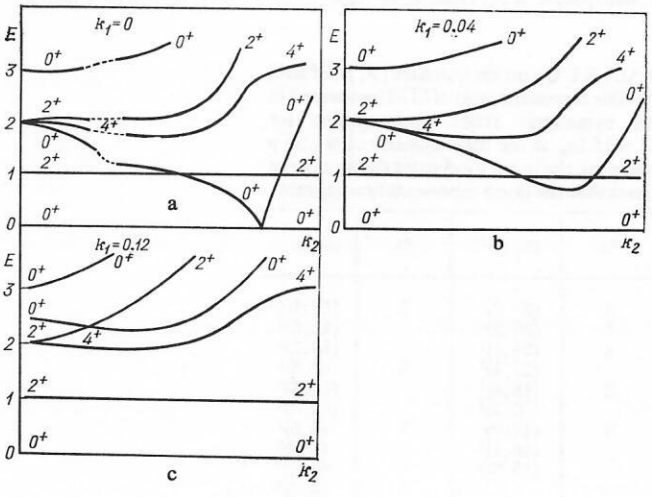

FIG. 1. Eigenvalue spectrum of the Hamiltonian (21) as a function of κ_2 for different κ_1.

The case of large values of the parameters $\varkappa_1$ and $\varkappa_2$ can be treated analytically, since for certain relationships between $\varepsilon, \varkappa_1, \varkappa_2, c_L$ the eigenvalues of the Hamiltonian (21) can be expressed in terms of the quantum numbers of a different chain of subgroups of SU(6):

$$SU(6) \supset SU(3) \supset O(3). \tag{26}$$

Then the Hamiltonian (21) can be expressed as follows [SU(3) limit of the IBM][1,6,17]:

$$H = -\varkappa \sum_{\nu} \tilde{Q}_{\nu}^{\dagger} \tilde{Q}_{\nu} + \varkappa' \hat{I}^2. \tag{27}$$

Here, $\hat{I}_{\nu} = \sqrt{10}(d^{+}d)_{\nu}^{(1)}$ is the angular-momentum operator, and

$$\tilde{Q}_{\nu} = d_{\nu}^{\dagger} s + s^{+} d_{\nu} \pm \frac{\sqrt{7}}{2} (d^{+}d)_{\mu}^{(2)}. \tag{28}$$

One can say that the five operators $\tilde{Q}_{\nu}$ and the three operators $\tilde{I}_{\nu}$ form the SU(3) algebra, and the Hamiltonian (27) is a linear combination of the Casimir operator of the group SU(3) and the square of the angular-momentum operator. The spectrum of eigenvalues of the Hamiltonian (27) has the form

$$E(I, \lambda, \mu) = -\varkappa(\lambda^2 + \mu^2 + \lambda\mu + 3\lambda + 3\mu) + \left(\frac{3}{4}\varkappa + \varkappa'\right) I(I+1). \tag{29}$$

Here, λ and λ are positive integers which characterize the irreducible representations of SU(3). It should be borne in mind that not all irreducible representations of SU(3) are realized as eigenfunctions of the Hamiltonian (27), but only those that belong to the completely symmetric representations of SU(6) characterized by the given value of Ω. In Table I, we list the representations belonging to the completely symmetric SU(6) representations for $\Omega = 15$.

As can be seen from (29), the eigenvalue spectrum of the Hamiltonian (27) consists of a set of rotational bands with the same moments of inertia constructed on different internal states. Each band is characterized by the quantum numbers (λ, λ, K). Here, K is an additional quantum number, equal to the minimal spin of the band. The number K is determined by the smaller of the numbers λ and λ. If, for example, $\lambda \leqslant \lambda$, then $K = \lambda, \lambda - 2, \ldots$. The spins in a band take the values $I = K, K+1, K+2, \ldots, K+\lambda$ for $K \neq 0$, but if $K = 0$, then $I = 0, 2, 4, \ldots, \lambda$. If $\lambda > \lambda$, then in these rules (Elliott's rules) for determining I the quantum numbers λ and λ are interchanged. We emphasize especially that, as can be seen from (29), the state energy does not depend on K.

TABLE I. Quantum numbers (λ, μ) of irreducible representations of SU(3) contained in the symmetric SU(6) representation for $\Omega = 15$ (n_b is the total number of β and γ phonons; the index ν indicates the number of times that the given representation occurs).

n_b	$(\lambda, \mu)^{\nu}$	n_b	$(\lambda, \mu)^{\nu}$
0	$(30,0)^1$	5	$(10,10)^1$
1	$(26,2)^1$		$(12,6)^2$
2	$(24,0)^1$		$(14,2)^2$
	$(22,4)^1$	6	$(8,8)^1$
3	$(18,6)^1$		$(10,4)^2$
	$(20,2)^1$		$(12,0)^2$
4	$(14,0)^1$	7	$(6,6)^1$
	$(16,4)^1$		$(8,2)^2$
	$(18,0)^1$		$(4,4)^1$
			$(6,0)^2$
			$(2,2)^1$
			$(0,0)^1$

The band with the lowest energy has the quantum numbers $(\lambda, \lambda, K) = (2\Omega, 0, 0)$. The next two bands are degenerate and have the quantum numbers $(\lambda, \lambda, K) = (2\Omega - 4, 2, 0)$ and $(2\Omega - 4, 2, 2)$. After this, if the values of Ω permit, comes a group of four bands with the quantum numbers $(2\Omega - 8, 4, 0)$, $(2\Omega - 8, 4, 2)$, $(2\Omega - 8, 4, 4)$, $(2\Omega - 6, 0, 0)$, etc. (Fig. 2).

If Ω is a sufficiently large number, the ratio of the energies of the bases of the first and second groups of bands is approximately equal to 2, and the spectrum in Fig. 2 can be interpreted in the framework of the traditional picture of the collective excitations of strongly deformed nuclei. The band with the lowest energy is constructed on the ground state. The band $(\lambda = 2\Omega - 4, \lambda = 2, K = 0)$ is constructed on a β-vibrational state, and the band $(\lambda = 2\Omega - 4, \lambda = 2, K = 2)$ on a γ-vibrational state. The quantum energies of the two vibrations are approximately the same and equal to

$$\omega_{\beta} = \omega_{\gamma} \simeq 12\Omega\varkappa.$$

The second group of bands is constructed on two-phonon states. There are either two β phonons ($K = 0$) or two γ phonons ($K = 0, 4$), or one β phonon and one γ phonon ($K = 2$). In the general case, one can show that if $\Omega \gg n_b$, where n_b is the total number of β and γ phonons, then the eigenvalue spectrum of the Hamiltonian is identical to the spectrum

$$E(n_{\beta}, n_{\gamma}, I) = E_0 + 12\Omega\varkappa(n_{\beta} + n_{\gamma}) + \left(\varkappa' + \frac{3}{4}\varkappa\right) I(I+1), \tag{30}$$

where n_{β} and n_{γ} are the numbers of β and γ phonons.

If it is assumed that the operator of the electric quadrupole moment is proportional to $\tilde{Q}_{\nu}$ (28), then the probabilities of $E2$ transitions between bands with different (λ, λ) will be zero. The probabilities of transitions between bands with the same (λ, λ) but different K remain indeterminate, since these bands are degenerate in the approximation under consideration. For transitions within the ground rotational band we obtain the expression

$$B(E2; I \to I') = 4(4\Omega^2 + 6\Omega + 3) \times (C_{I020}^{I'0})^2 \left\{1 - \frac{1}{2} \frac{I(I+1) + I'(I'+1)}{4\Omega^2 + 6\Omega + 3}\right\}, \tag{31}$$

where $C_{I020}^{I'0}$ is a Clebsch-Gordan coefficient. For $I^2 \ll 4\Omega^2$, this expression gives Alaga's rules for the probabilities of $E2$ transitions.

Thus, the Hamiltonian (21) contains as special cases solutions corresponding to the model of harmonic quadrupole vibrations and the model of an axisymmetric rotator that makes small vibrations about its equilibrium shape.

The energy spectra behave differently for $\varkappa_2 = 0$ and increasing $\varkappa_1$. In this case, the eigenvalue spectrum is identical to the spectrum of collective excitations in the Jean-Wilets model[18] (Fig. 3). For $\varkappa_2 = 0$, the seniority is a good quantum number, and the eigenvalue spectrum is degenerate with

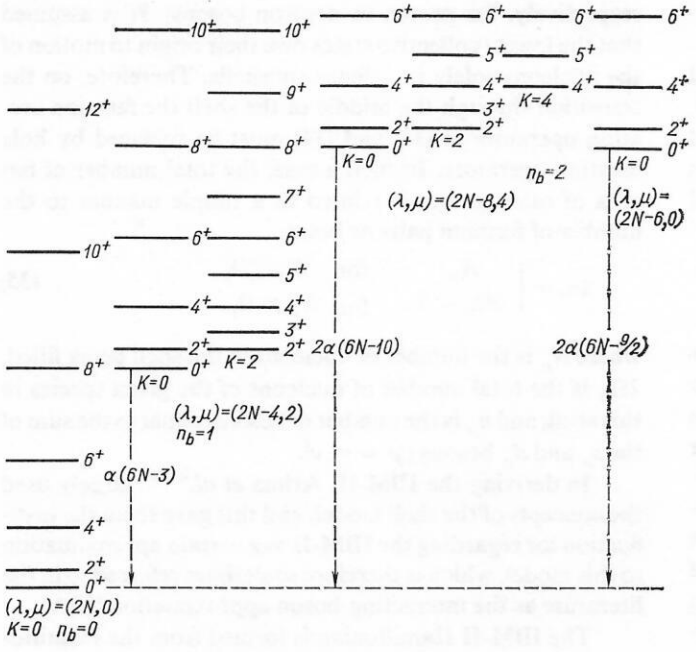

FIG. 2. Spectrum of energy states in the SU(3) limit.

respect to it. With increasing $\varkappa_1$, the deviation from equidistance increases and overall the spectrum behaves as in the generalized nuclear model with increasing rigidity of the β vibrations. Thus, the parameter $\varkappa_1$ in the interacting-boson model plays the same role as the parameter $\langle\beta^2\rangle$ in the collective Bohr-Mottelson model.

Among the experimentally investigated nuclei there are some whose spectrum of excited states agrees well with the predictions of the model for $\varkappa_2 = 0$. These are nuclei with highly excited 0_2^+ states and almost degenerate 2_2^+ and 4_1^+ levels. They are found in the region of the isotopes Ba, Hg, and Pt. Calculations of the deformation potential energy confirm its weak dependence on γ.

For $\varkappa_2 = 0$, there exists a set of parameters $\varepsilon, \varkappa_1, c_L$ for which the Hamiltonian (21) can be expressed in terms of the Casimir operators of one further chain of SU(6) subgroups[19]:

$$SU(6) \supset O(6) \supset O(5) \supset O(3). \qquad (32)$$

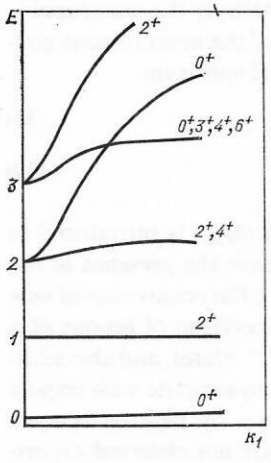

FIG. 3. Dependence of the state spectrum of the Hamiltonian (21) on $\varkappa_1$ for $\varkappa_2 = 0$.

In this case, the problem can also be solved analytically [$O(6)$ limit of the IBM].

Thus, the interacting-boson model describes the transition from spherical to deformed nuclei. It is in this that it differs from many other models. The transition itself can be made differently, depending on the behavior of the coefficients $\varkappa_1$ and $\varkappa_2$:

a) if $\varkappa_1$ and $\varkappa_2$ increase simultaneously, then there is a smooth transition from a vibrational to a rotational spectrum;

b) for small $\varkappa_1$ and a rapid growth in $\varkappa_2$, low-lying 0^+ states arise in the transitional region, and these can even sink below the 2_1^+ states;

c) at values of $\varkappa_2$ near zero and increasing $\varkappa_1$, the energy of the 0_2^+ state increases sharply. The energies of the 2_2^+ and 4_1^+ states are nearly the same, and the ratio of their energies to the energy of the 2_1^+ state is in the interval 2.0–2.5.

As follows from the above, the results to which the IBM leads are in many respects very close to the results of the Bohr-Mottelson model (BMM). This is not surprising, since the physical foundations of the two models are the same—both models treat the lowest collective states as the manifestation of five quadrupole degrees of freedom.

Both models are based on the assumption of a weak coupling of a collective quadrupole degree of freedom to the other degrees of freedom of the nucleus. Indeed, it was on the basis of this assumption that Hamiltonians containing only collective quadrupole operators were constructed. The main difference between the IBM Hamiltonian and the BMM Hamiltonian is that the former is represented by a finite matrix in the boson space. This greatly simplifies the problem of diagonalizing the Hamiltonian but does not, we believe, have a deep physical basis, being rather a consequence of the approximations made in the derivation of the interacting-boson model.

In some cases, for example, when the number Ω is large

(as is the case in stably deformed nuclei), the IBM Hamiltonian can be reduced to the standard BMM Hamiltonian (quadratic function of the collective momenta plus a potential energy as a function of the collective coordinates β and γ). The first discussion of the relationship between the IBM and the BMM was in Refs. 5 and 14; many other discussions followed.[11,20–27] In Sec. 8 we shall consider in more detail some of the questions discussed in these studies.

3. MODEL OF INTERACTING PROTON AND NEUTRON BOSONS (IBM-II)

Experimental data have been analyzed widely by means of the second variant of the interacting-boson model—the IBM-II, in which two species of bosons are used: neutron and proton bosons. The basis for the doubling in the number of bosons was the desire to separate explicitly in the collective Hamiltonian the proton-neutron interaction. The important part which it plays is revealed, for example, in the way the nuclear spectra change with increasing number of nucleons of one species. Indeed, the spectra of nuclei in which the number of protons (or neutrons) is equal to a magic number change their nature only slightly with increasing number of valence neutrons (respectively, protons), remaining close to the spectrum of a weakly anharmonic vibrator. But the addition of, for example, a pair of protons in the case of $_{50}$Sn above the closed shells greatly reduces the energy of the first 2_1^+ level, and when the number of protons is further increased the spectrum acquires a rotational nature.

The explicit separation of the proton-neutron interaction in the collective Hamiltonian by the introduction of proton and neutron bosons was proposed by Arima, Iachello, Otsuka, and Talmi.[28–30] The IBM-II was formulated on the basis of the assumption that the lowest collective states are formed from collective fermion pairs bound to give angular momenta of zero and two. Arima *et al.* used a variant of microscopic theory in which the basis states of even systems are constructed on the basis of the function

$$[\sum_j \psi_j^{(0)} (a_j^+ a_j^+)^{(0)}]^{N/2} \mid 0\rangle = [S^+]^{N/2} \mid 0\rangle \tag{33}$$

(N is the number of fermions), which is proportional to the Bardeen–Cooper–Schrieffer function projected onto a definite number of particles (N in the given case). The function (33) is represented as a power of the operator that generates the most strongly bound pair of fermions having zero angular momentum (S pair). In such a construction of the theory, the functions of the collective states are superpositions of (33) and the functions obtained by replacing one or several S pairs in (33) by a corresponding number of D pairs:

$$D_\mu^+ = \sum_{j_1 j_2} \psi_{j_1 j_2}^{(2)} (a_{j_1}^+ a_{j_2}^+)_\mu^{(2)}. \tag{34}$$

It was shown in Refs. 28–30 that the amplitudes $\psi_j^{(0)}$ and $\psi_{j_1 j_2}^{(2)}$ in (33) and (34) can be found by diagonalizing the fermion Hamiltonian of the shell model, which includes an average field and residual interactions.

The S and D pairs are introduced separately for the protons and neutrons, and then the states constructed from them are mapped to boson wave functions constructed from scalar, s_ρ, and quadrupole, $d_{\rho\lambda}$, bosons (ρ is equal to π or ν, respectively, for proton or neutron bosons). It is assumed that the lowest collective states owe their origin to motion of the nucleons solely in valence subshells. Therefore, on the transition through the middle of the shell the fermion creation operators in (33) and (34) must be replaced by hole creation operators. In such a case, the total number of bosons of each species is related in a simple manner to the number of fermion pairs or holes:

$$2n_\rho = \begin{cases} N_\rho & \text{for } N_\rho \leqslant \Omega_\rho, \\ 2\Omega_\rho - N_\rho & \text{for } N_\rho > \Omega_\rho, \end{cases} \tag{35}$$

where N_ρ is the number of nucleons in the shell being filled, $2\Omega_\rho$ is the total number of nucleons of the given species in this shell, and n_ρ is the number of bosons, equal to the sum of the s_ρ and d_ρ bosons ($\rho = \pi, \nu$).

In deriving the IBM-II, Arima *et al.*[28–30] largely used the concepts of the shell model, and this gave them the justification for regarding the IBM-II as a certain approximation to this model, which is therefore sometimes referred to in the literature as the interacting-boson approximation (IBA).

The IBM-II Hamiltonian is formed from the Hamiltonians for the bosons of each species separately and the interaction between the proton and neutron bosons ($V_{\pi\nu}$):

$$H \text{ (IBM-II)} = \sum_{\rho=\pi,\ \nu} H_\rho = V_{\pi\nu}. \tag{36}$$

Formally, H_ρ is like H (IBM-I) (21), in which all the operators are for bosons of type ρ. However, for H_ρ a somewhat simpler expression is chosen:

$$H_\rho = e_{d\rho} \hat{n}_{d\rho} + \frac{1}{2} \sum_{L=0,\ 2,\ 4;\ \mu} c_{L\rho} (d^+ d^+)_{\rho\mu}^{(L)} (dd)_{\rho\mu}^{(L)}, \tag{37}$$

since the Hamiltonian (37), as was shown above (see Sec. 2), makes it possible to reproduce the spectrum of a weakly anharmonic vibrator, which is characteristic of nuclei with a closed proton or neutron shell. The form (37) for H_ρ is evidently too strongly simplified. In Ref. 31, arguments are given for including in H_ρ terms that do not conserve the number of d bosons (quadrupole–quadrupole interaction between identical bosons).

In establishing the form of $V_{\pi\nu}$, allowance is made, first, for the well-known fact that it is precisely the quadrupole–quadrupole interaction that is one of the main reasons governing the appearance of a rotational spectrum:

$$V_{\pi\nu} = -k \sum_\mu Q_{\pi\mu}^+ Q_{\nu\mu} + M_{\pi\nu}; \tag{38}$$

$$Q_{\rho\mu} = (d_\mu^+ s + s^+ d_\mu^-)_\rho + \chi_\rho (d^+ d)_{\rho\mu}^{(2)}. \tag{39}$$

Second, a so-called Majorana term ($M_{\pi\nu}$) is introduced in $V_{\pi\nu}$. This term appears in $V_{\pi\nu}$ because the presence of bosons of two species (π and ν) leads to the occurrence of new states that are not present in the spectrum of bosons of a single species, in particular, $I^\pi = 1^+$ states, and also additional $I^\pi = 2^+$ states, which are not symmetric with respect to the replacement of proton bosons by neutron bosons. Since such states with low energy are not observed experimentally, $M_{\pi\nu}$ is constructed in such a way as to ensure a raising of the energies of such states:

$$M_{\pi\nu}=\xi^{(2)}\sum_{\mu}(d^{+}_{\pi\mu}s^{+}_{\nu}-d^{+}_{\nu\mu}s^{+}_{\pi})(d_{\pi\mu}s_{\nu}-d_{\nu\mu}s_{\pi})$$
$$+\sum_{L=1,\,3;\,\mu}\xi^{(L)}(d^{+}_{\pi}d^{+}_{\nu})^{(L)}_{\mu}(d_{\pi}d_{\nu})^{(L)}_{\mu},\quad \xi^{(L)}>0. \tag{40}$$

It follows from (37), (38), and (40) that the total number of parameters of the IBM-II Hamiltonian reaches 14:

$$e_{\pi d},\ c_{L\pi},\ e_{\nu d},\ c_{L\nu},\ k,\ \chi_{\pi},\ \chi_{\nu},\ \xi^{(1)},\ \xi^{(2)},\ \xi^{(3)}.$$

This number is too large for phenomenological analysis, and therefore the following simplifications are introduced. In the analysis of a chain of isotopes (Z fixed) one takes $\xi^{(L)}=\xi$, $c_{L\pi}$ (frequently, $c_{L\pi}=0$), χ_{π} to be the same for the complete chain. Then for each nucleus one chooses $e_{\pi d}=e_{\nu d}=\varepsilon$, $k,\chi_{\nu},c_{\nu L}$ (frequently, one sets $c_{2\nu}=c_{4\nu}=0$). In the analysis of a chain of isotones (N fixed), the neutron parameters are kept constant. Finally, for each nucleus one varies about four parameters, and for the complete group of isotopes (or isotones) a further 2–3 parameters, so that the total number of parameters is approximately equal to 7, i.e., about the same as in the IBM-I.

The $E2$-transition operator is constructed from the operators Q_{ρ} (39) and in principle must include four parameters: two effective charges (proton and neutron) and two values of $\chi_{\rho E2}$. However, it is usually assumed that the parameters χ_{ρ} in the Hamiltonian (36) and in the $E2$-transition operator are the same:

$$\hat{T}_{\mu}(E2)=\sum_{\rho}e^{*}_{\rho}[(d^{+}_{\mu}s+s^{+}\tilde{d}_{\mu})_{\rho}+\chi_{\rho}(d^{+}d)^{(2)}_{\rho\mu}]. \tag{41}$$

The IBM-II wave functions are constructed as vector products of boson proton and neutron functions. As a result, the IBM-II basis is usually much larger than the IBM-I basis. (For example, for two proton and two neutron bosons we have 65 states, whereas for four identical bosons there are only 18.) This fact alone shows that the IBM-II must include the IBM-I.

In Refs. 28–30 it was shown that the transition from the IBM-II to the IBM-I can be made by projecting the IBM-II functions onto states that are completely symmetric with respect to the proton and neutron bosons, this being equivalent to the separation in the IBM-II Hamiltonian of the terms that possess the same symmetry.

The separation of symmetric boson configurations is not the only way of making the transition from the IBM-I to the IBM-II. We consider, for example, the following possibility. By means of a unitary transformation, we eliminate the s bosons, this being equivalent to a transition to a particle-hole picture for describing collective states.[10,11] We then go over from the d_{π}^{+} and d_{ν}^{+} bosons to the operators $d^{+}=\sqrt{\Omega_{\pi}/\Omega}\,d_{\pi}^{+}+\sqrt{\Omega_{\nu}/\Omega}\,d_{\nu}^{+}$ and $d'^{+}=\sqrt{\Omega_{\nu}/\Omega}\,d_{\pi}^{+}-\sqrt{\Omega_{\pi}/\Omega}\,d_{\nu}^{+}$ ($\Omega=\Omega_{\pi}+\Omega_{\nu}$). The strong proton-neutron quadrupole-quadrupole Majorana interaction (38), (40) lowers the energy of the d boson and raises the energy of the d' boson. Thus, it can be assumed that the d boson corresponds to the most collective superposition of particle-hole pairs, and the d' to weakly collectivized pairs. Ignoring the d' bosons in the transformed Hamiltonian, we obtain the IBM-I in the form (9). This argument shows that the introduction of the proton and neutron bosons in the IBM-II takes into account the coupling of the most collectivized states to states of other kinds. Allowance for these states can be important in the cases when the collective mode is insufficiently separated from the other states (as can happen, for example, when the nucleus is nearly magic with respect to one species of particle). In addition, the coupling to the d' states, in which the protons and neutrons move in antiphase, evidently takes into account effectively the coupling to the isovector quadrupole resonance, this having a smoothing effect on the variation of the parameters of the model with increasing number of nucleons of one species.

The boson Hamiltonian IBM-II (36) and the operator (41) of the quadrupole transition are constructed from the generators of the proton and neutron SU(6) groups:

$$d^{+}_{\rho\mu}s_{\rho},\ s^{+}_{\rho}d_{\rho\mu},\quad d^{+}_{\rho\mu}d_{\rho\nu}-\delta_{\mu\nu}s^{+}_{\rho}s_{\rho}. \tag{42}$$

Therefore, the dynamical symmetry group of the IBM-II is the direct product $SU^{(\pi)}(6)\times SU^{(\nu)}(6)$. The further classification of the proton and neutron states separately can be done in the same way as in the IBM-I, i.e., by means of the three chains of subgroups (25), (26), and (32). Besides this, the entire proton-neutron function can be characterized by the quantum numbers of a group that unifies the proton and neutron symmetry groups. This unifying group necessarily has the group of three-dimensional rotations $O(3)$ as a subgroup, since every physical state has a definite angular momentum and projection of it.

We now give these possible chains of subgroups[31,32]:

$$SU^{(\pi)}(6)\times SU^{(\nu)}(6)$$
$$\left\{\begin{array}{ll}\supset SU^{(\pi)}(5)\times SU^{(\nu)}(5)\supset SU(5)\supset O(5)\supset O(3); & (43)\\ \supset SU^{(\pi)}(3)\times SU^{(\nu)}(3)\supset SU(3)\supset O(3); & (44)\\ \supset O^{(\pi)}(6)\times O^{(\nu)}(6)\supset O(6)\supset O(5)\supset O(3). & (45)\end{array}\right.$$

The function of an irreducible representation of a proton or neutron group separately is completely symmetric. However, among the functions of irreducible representations that unify the groups SU(5) and $O(6)$ and appear in (43) and (45) there are not only completely symmetric functions (these functions describe, as before, the states with the lowest energy) but also functions of intermediate symmetry. Such functions are characterized by Young diagrams with two rows.

The SU(3) representations that occur in (44) are also distinguished from the representations obtained on the reduction of the completely symmetric SU(6) function in the IBM-I. In the present case, besides diagrams with (λ,λ), where λ and λ are even numbers (Table I), there are diagrams with odd values of λ and λ, for example, $\lambda=2(n_{\pi}+n_{\nu})-2$, $\lambda=1$. The states belonging to this representation give a band with $K=1$ [the reasons for the appearance of the states with $I^{\pi}=1^{+}$ were discussed above in connection with the introduction of the Majorana forces (40)].

As in the case of the IBM-I, analytic solutions of the IBM-II Hamiltonian are possible in the cases when, with definite relationships between the parameters, the IBM-II Hamiltonian reduces to a sum of the Casimir operators of subgroups in a corresponding chain. It is obvious that for

values of ε much greater than k and $c_{\rho L}$ we shall have a spectrum that is nearly harmonic [SU(5) limit of the IBM-II (43)]. In the case $\varepsilon \simeq 0$, the situation depends on χ_ρ. If $\chi_\pi \simeq \chi_\nu \simeq 0$, the spectrum will have features found in a γ-unstable rotator [$O(6)$ limit of the IBM-II (45)]. For $|\chi_\pi| \simeq |\chi_\nu| \simeq \sqrt{7}/2$ we obtain the SU(3) limit of the IBM-II (44). As is pointed out in Ref. 31, there are here two possibilities. First, if χ_π and χ_ν have the same sign, then the functions of the lowest states are described by diagrams like those considered in the IBM-I (see Sec. 2). Second, it may happen that χ_π and χ_ν have opposite signs. Such a situation can arise if the neutrons, for example, begin to fill a shell at the same time that the protons begin to close a shell. Then a difference in the signs of χ_ρ follows from the simplified model, in which the real levels of the subshells are replaced by one degenerate level with degeneracy $2\Omega_\rho = \Sigma_i(2j_i + 1)$. In this model [see (52) in Sec. 5], the quantity χ_ρ is proportional to $\Omega_\rho - N_\rho$, i.e., this model predicts a change in the sign of χ_ρ on the transition of the number of nucleons (N_ρ) through the middle of the shell. If in this case we assume, for example, for the neutron function of the lowest state the scheme $SU^{(\nu)}(3)$ ($\lambda = 2n_\nu$, $\lambda = 0$), then the proton function of the lowest state (because of the opposite sign of χ_π) must have $SU^{(\pi)}(3)$ ($\lambda = 0$, $\lambda = 2n_\pi$), i.e., must be described by the conjugate representation. In this case, such representations appear in the same way as in the classification of elementary particles, when the particles and antiparticles are placed in conjugate representations. The analogy with the IBM takes a form in which the particles correspond to the bosons to which the nucleon pairs that begin to fill the shell are mapped, while the antiparticles correspond to the bosons corresponding to hole pairs, i.e., the nucleons lacking from shell completion.

Besides the representations mentioned above, there are contained in $SU^{(\rho)}$ (6) other representations of $SU^{(\rho)}$ (3), these being similar to the ones described in Sec. 2 (with even values of λ and λ), the numbers λ and λ being interchanged for the conjugate schemes. The direct product of such representations gives the following values of (λ, λ) for the unifying SU(3), which Dieperink and Bijker[31] suggest should be denoted by SU*(3):

$$(2n_\nu,\ 2n_\pi);\ (2n_\nu - 4,\ 2n_\pi + 2);\ (2n_\nu + 2,\ 2n_\pi - 4);$$
$$(2n_\nu - 1,\ 2n_\pi - 1)\ \ldots \qquad (46)$$

If the IBM-I Hamiltonian is to be representable as the SU*(3) Casimir operator, the Hamiltonians describing the proton and neutron bosons separately must contain a quadrupole-quadropole interaction. If this is the case, then the spectrum is given by the eigenvalues of the Casimir operator (29). It is shown in Ref. 31 that for SU*(3) the spectrum of the lowest states is remarkably similar to the spectrum of a rigid nonaxial rotator with $\gamma = 30°$. At the same time, as can be seen from (46), the spectrum of excited states contains very naturally states with $I^{(\pi)} = 0^+$, which are absent in the rotator spectrum (see Fig. 4, which shows the lower part of the SU*(3) spectrum for $n_\pi = 3$ and $n_\nu = 4$ from Ref. 31).

Thus, in the IBM-II there is a possibility of describing nonaxial nuclei together with γ-unstable nuclei, whereas the IBM-I describes only the latter. Note that in principle non-

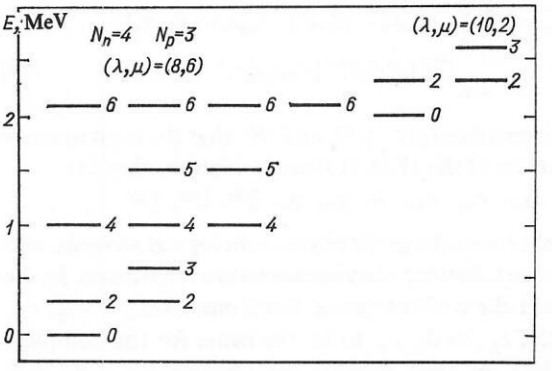

FIG. 4. Spectrum of energy states in the SU*(3) limit of the IBM-II ($\chi_\pi = -\chi_\lambda$) in accordance with the data of Ref. 31.

axiality could be introduced in the IBM-I by adding to the Hamiltonian terms that take into account a three-boson interaction of the type $\Sigma_\lambda (d^+d^+d^+)^{(L)}_\lambda (ddd)^{(L)}_\lambda$, where $L = 0$, 3, 4, 6.[22,25]

4. USE OF THE IBM TO DESCRIBE THE PROPERTIES OF Ru AND Pd ISOTOPES

As an example of calculations of the structure of low collective states, we consider the results for the isotopes $_{44}$Ru and $_{46}$Pd obtained in the framework of the IBM-II in Ref. 33.

Figure 5 shows the calculated and experimental energies of the states of the ground-state bands of Ru and Pd. It can be seen that there is good agreement between the calculations (curves) and experimental results (points), but the energies of the high-spin states of the nuclei with N equal to 54 and 56 differ from the experimental values. This is an indication of a possible two-quasiparticle nature of these states or a significant admixture of such states. This is also indirectly indicated by the appearance of the maximum at $N = 58$.

Figure 6 shows the energies of the levels of the β and γ bands of the Ru and Pd isotopes. It can be seen that the calculated energies of the 0_2^+ states of Ru with N equal to 56 and 58 are too high.

Figure 7 shows the values of the parameters ε and k, and Fig. 8 shows the values of the parameters χ_ν and also $c_{\nu L}$. The values of χ_π are 0.4 for Ru and 0.2 for Pd. The values of χ_ν for the Ru and Pd isotopes with the same numbers of neutrons are taken to be the same. This also holds for the values of $c_{\nu L}$. The terms of the Hamiltonian proportional to $c_{\nu L}$ have little effect on the results of the calculation, and we therefore concentrate our attention on the parameters ε, k, χ_ν. It can be seen that the parameters ε and k change little with varying number of neutrons and, moreover, are approximately the same for Ru and Pd. The parameter χ_ν changes appreciably. For $N \geqslant 60$, it varies approximately linearly with increasing number of neutrons, and at $N = 70$ it changes sign.

Besides the calculations of the energies, the absolute values of the reduced probabilities of $E2$ transitions were calculated in Ref. 33. The boson operator of the $E2$ transition was taken to be the operator $\hat{T}(E2)$ (41) with the same values of the parameters χ_π and χ_ν as were found to be opti-

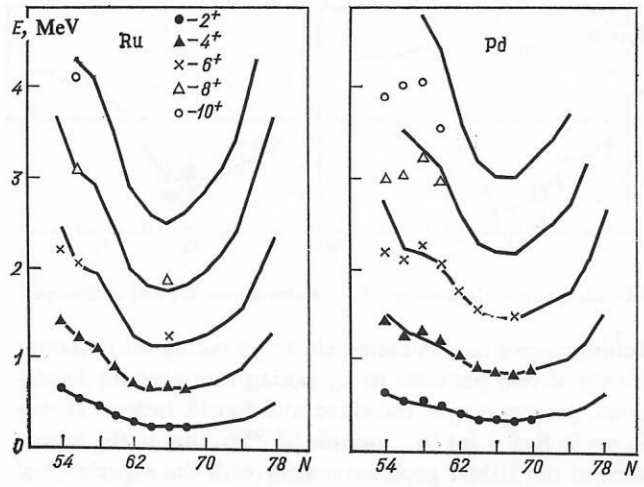

FIG. 5. Theoretical curves and experimental values of the state energies of the ground-state band of the isotopes $_{44}$Ru and $_{46}$Pd.

mal for the calculation of the energies. For simplicity, it was assumed that $e_\pi^* = e_\nu^* = e^*$. The values of e^* were chosen on the basis of the experimental $B(E2; 2_1^+ \to 0_1^+)$ values in ^{98}Ru and ^{102}Pd. The values of e^* chosen in this manner were found to be very similar: 0.103 and 0.105e·b. For these values of e^*, the reduced probabilities of $E2$ transitions in the Ru and Pd isotopes are enhanced compared with the single-particle estimate by about n times (n is the number of bosons).

Figure 9 gives the calculated and experimental values of $B(E2)$ for the $2_2^+ \to 0_1^+$ and $4_1^+ \to 2_1^+$ transitions in Ru and Pd. Figure 10 gives the values of $B(E2)$ for the $2_2^+ \to 0_1^+$ transitions, and Fig. 11 gives the values of $B(E2)$ for the $2_2^+ \to 0_1^+$ and $2_1^+ \to 0_2^+$ transitions. It can be seen that there is good agreement between the results of the theory and experiment. An exception is the values of $B(E2; 2_2^+ \to 0_1^+)$ in the Pd isotopes, and also the $B(E2; 2_1^+ \to 0_2^+)$ values for the Ru isotopes with N equal to 56 and 58. This fact and the disagreement between the calculated and experimental energies of the 0_2^+ states suggest to the authors that the 0_2^+ states of these isotopes have a particular noncollective nature.

The results of the comparison of the experimental and calculated values of the quadrupole moments $Q(2_1^+)$ of the 2_1^+ states of the Ru and Pd isotopes are given in Fig. 12 in

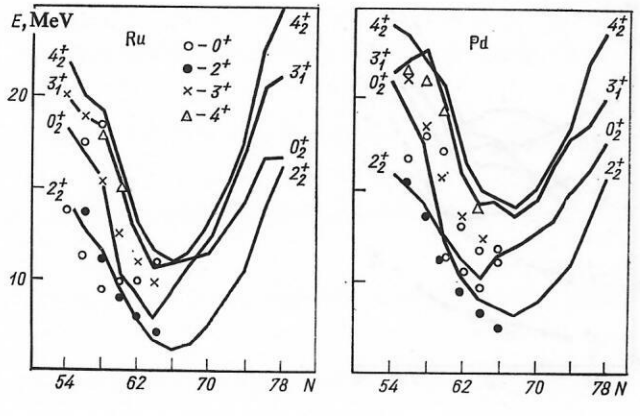

FIG. 6. Energies of the states of the β and γ bands of Ru and Pd isotopes.

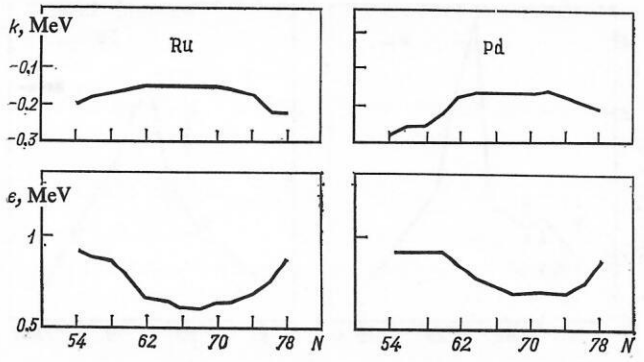

FIG. 7. Dependence of the parameters ε and k on the number of neutrons for the Ru and Pd isotopes.

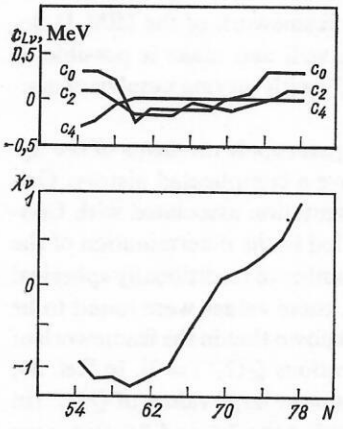

FIG. 8. Dependence of the values of the parameters χ_ν and $c_{\nu L}$ on the number of neutrons for the Ru and Pd isotopes.

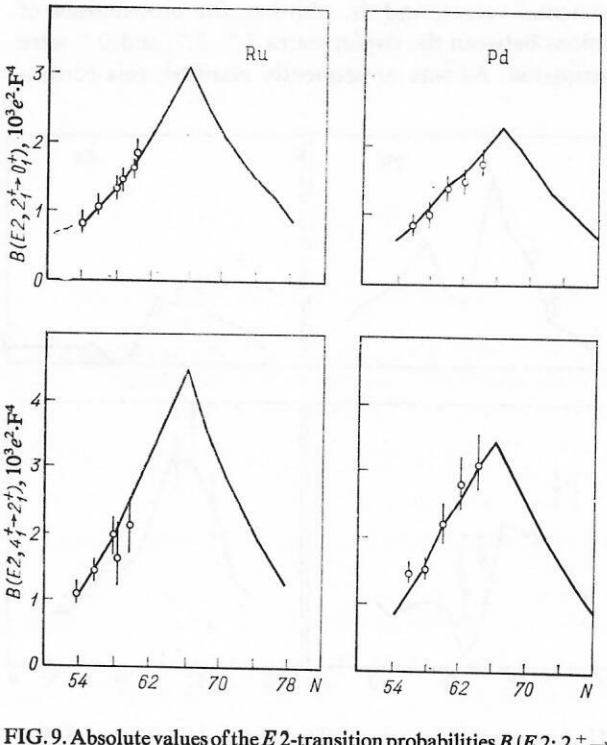

FIG. 9. Absolute values of the $E2$-transition probabilities $B(E2; 2_1^+ \to 0_1^+)$ and $B(E2; 4_1^+ \to 2_1^+)$ for the Ru and Pd isotopes.

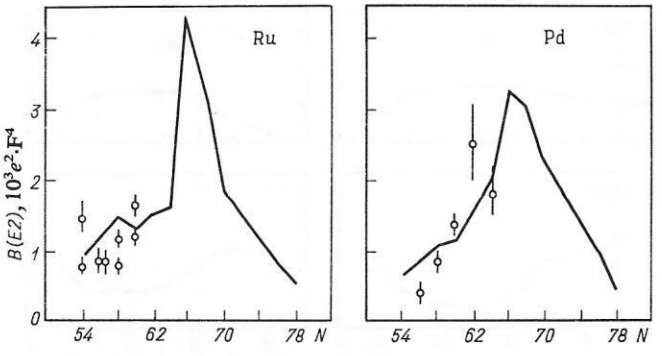

FIG. 10. Absolute $E2$-transition probabilities $B(E2; 2_2^+ \to 2_1^+)$ for Ru and Pd isotopes.

accordance with the data of Ref. 33. It can be seen that the calculations of $Q(2_1^+)$ in the framework of the IBM-II describe the experimental data well and make it possible to describe the variation of $Q(2_1^+)$ with varying number of neutrons.

The calculations of the quadrupole moments of the 2_1^+ states of even-even nuclei have a complicated history. Originally, experiments on reorientation associated with Coulomb excitation of 2_1^+ levels led to the determination of the values of $Q(2_1^+)$ for a large number of traditionally spherical nuclei. In a number of cases, these values were found to be unexpectedly large [it is well known that in the framework of the concept of harmonic vibrations $Q(2_1^+) = 0$]. In Ref. 34, an attempt was made to explain the large values of $Q(2_1^+)$ in spherical nuclei by proposing that the 2_1^+ and 2_2^+ states are mixtures of single- and two-phonon components. However, under this assumption the calculated values of the ratio $B(E2; 2_2^+ \to 0_1^+)/B(E2; 2_1^+ \to 0_1^+)$ appreciably exceeded the experimental values, and, in addition, the probabilities of transitions between the triplet states 4_1^+, 2_2^+, and 0_2^+ were overestimated. As was subsequently clarified, this contradiction cannot be eliminated either by taking into account mixing of two phonons or by taking into account anharmonic corrections of the third and fourth orders. It was shown in Ref. 1 for the example of ^{108}Pd that in the framework of the IBM-I good agreement with the experimental $B(E2)$, $Q(2_1^+)$ values and the energies of the excited states can be achieved simultaneously.

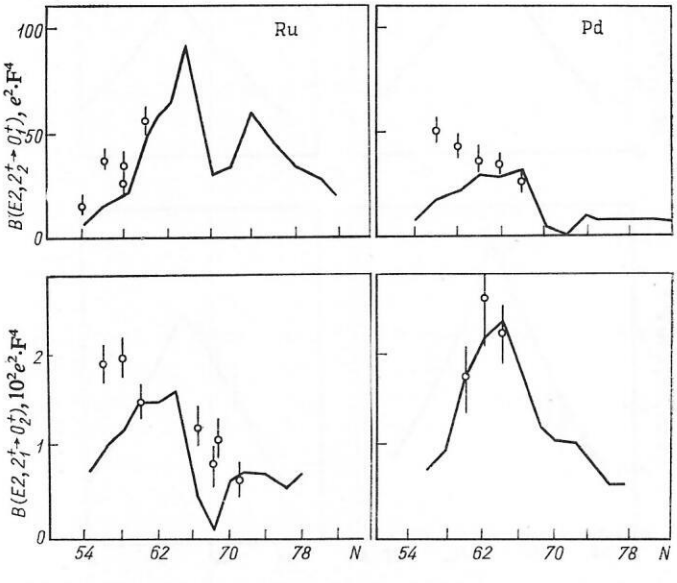

FIG. 11. Absolute transition probabilities $B(E2; 2_2^+ \to 0_1^+)$ and $B(E2; 2_1^+ \to 2_2^+)$ for Ru and Pd isotopes.

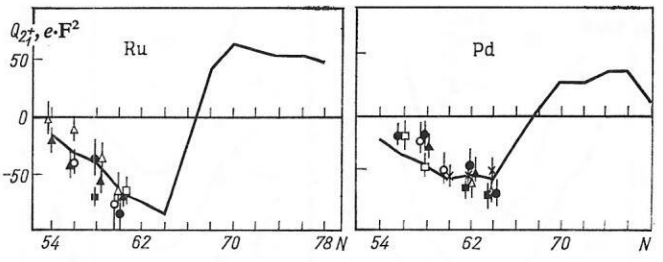

FIG. 12. Quadrupole moments of 2_1^+ states of even Ru and Pd isotopes.

5. CALCULATIONS OF COLLECTIVE STATES OF THE ISOTOPES Xe, Ba, Ce, Sm. THE EFFECTIVE NUMBER OF PROTON BOSONS FOR NUCLEI WITH Z = 50–64

In Ref. 35, the IBM-II was used to calculate the collective states of the Xe, Ba, and Ce isotopes. Figure 13 shows the calculated and experimental energies of the excited states of the Ba isotopes. For $N = 66$, the energies of the levels of the ground-state band vary approximately in accordance with the law $I(I+1)$, while the 0_2^+ and 2_2^+ levels are situated much higher. Such a situation is typical of nuclei with a potential energy that does not depend on the nonaxiality parameter γ (the so-called γ-unstable nuclei), and, as can be seen from Fig. 13, the IBM copes well with the description of the gradual transition from γ-unstable nuclei to nuclei whose properties approximate those of an axial rotator.

Figure 14a shows the phenomenological values of the parameters ε, k, χ_ν determined from an analysis of the energies of the collective states of the Ba, Ce, and Xe isotopes. Figure 14b gives the arbitrarily normalized values of the same parameters calculated in the approximation of a single degenerate level.[28–30] We explain the behavior of the curves in Fig. 14b using a rather elementary estimate for the dependence of the parameters on the number of particles on the basis of the quasiparticle approximation.[10] For this, we ap-

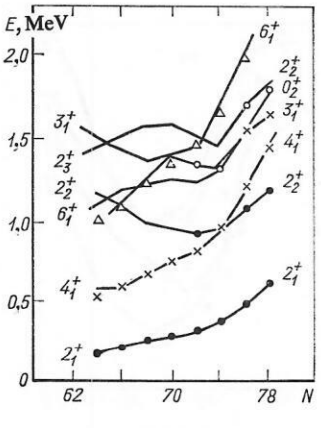

FIG. 13. Energies of excited states of Ba isotopes.

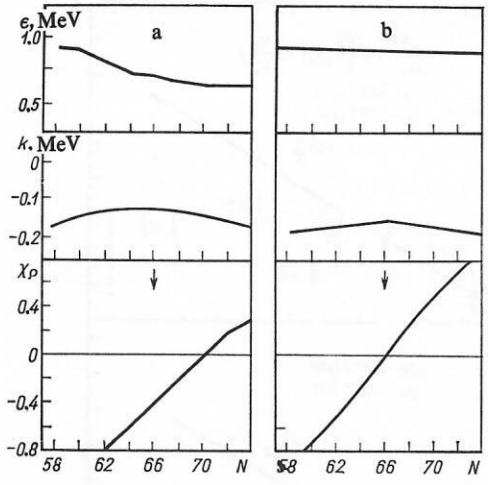

FIG. 14. Phenomenological values of the parameters ε, k, χ_ρ extracted from the energies of collective Ba, Ge, Xe states (a) and the arbitrarily normalized values of the same parameters obtained from the data of a microscopic calculation made in the approximation of one j level (b).

proximate the ground-state function of an even number (N) of nucleons in one level with degeneracy $2\Omega \gg 1$ by a quasiparticle vacuum function $|0\rangle \sim (s^+)^n |0)$. In such a simplified model, the Bogolyubov parameters can be determined directly:

$$u^2 = (2\Omega - N)\ (2\Omega)^{-1};\ v^2 = N\ (2\Omega)^{-1}. \tag{47}$$

We associate the state $(\alpha^+\alpha^+)^{(2)}|0\rangle$ with one quasiparticle pair with the boson function $d^+(s^+)^{n-1}|0)$. We compare the values of the matrix elements of the quadrupole operator in the fermion and boson spaces:

$$Q_\mu = \frac{\langle j \| Q \| j \rangle}{\sqrt{5}} \{(u^2 - v^2)\ (\alpha^+\alpha)^{(2)}_\mu - uv\ [(\alpha^+\alpha^+)^{(2)}_\mu + (\alpha\alpha)^{(2)}_\mu]\}$$
$$\to q_0\ (d^+_\mu s + s^+ d_{\bar{\mu}}) + q_1\ (d^+ d)^{(2)}_\mu. \tag{48}$$

It follows from (48) that the matrix element of the transition $|0\rangle \to (\alpha^+\alpha^+)^{(2)}|0\rangle$ is proportional to $uv \sim \sqrt{(2\Omega - N)N}$, and the corresponding matrix element in the boson space $[(s^+)^n|0) \to d^+(s^+)^{n-1}|0)]$ is proportional to $q_0\sqrt{n}$. With allowance for the correspondence rule (35) between the number of bosons and the number of fermions, we find that

$$q_0 \sim \sqrt{\Omega - n}. \tag{49}$$

The matrix element of the transition without change in seniority, $((\alpha^+\alpha^+)^{(2)}|0\rangle \to (\alpha^+\alpha^+)^{(2)}|0\rangle)$, depends on the number of particles through the factor $(u^2 - v^2) \sim (\Omega - N)$, whereas the corresponding boson matrix element is proportional to q_1, i.e.,

$$q_1 \sim (\Omega - N). \tag{50}$$

The dependence of the parameters k and χ_ρ on the number of particles can be established from (49) and (50). The parameter k is proportional to the product of the proton and neutron parameters:

$$k \sim q_{0\pi} q_{0\nu} \sim [(\Omega_\pi - n_\pi)\ (\Omega_\nu - n_\nu)]^{1/2}. \tag{51}$$

The resulting relation shows that for a fixed number of proton bosons, n_π, for example, the modulus of k decreases as the number of neutrons approaches the middle of the shell [$N_\nu = 0 \to n_\nu = 0$; $N_\nu = \Omega_\nu$ (middle of shell) $\to n_\nu = \Omega_\nu/2$;

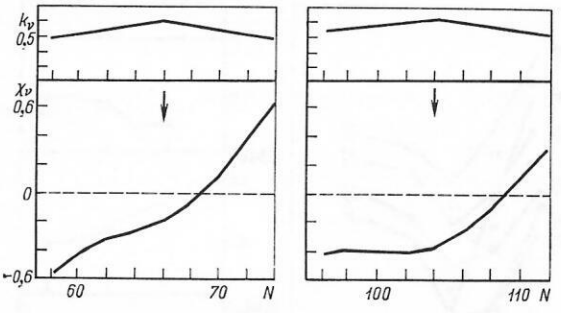

FIG. 15. Values of the parameters k_ν and χ_ν in accordance with a microscopic calculation made under the assumption of two degenerate j levels.

$N_\nu = 2\Omega_\nu \to n_\nu = 0$].

The parameter χ_ρ is determined by the ratio of $q_{1\rho}$ to $q_{0\rho}$:

$$\chi_\rho = \frac{q_{1\rho}}{q_{0\rho}} \sim \frac{\Omega_\rho - N_\rho}{\sqrt{\Omega_\rho - n_\rho}}. \tag{52}$$

Thus, in the approximation of one degenerate level the parameter χ_ρ changes sign in the middle of the shell (arrows in Fig. 14b), whereas the phenomenological value changes sign at larger values of the neutron number (Fig. 14a). Figure 15 shows how χ_ν changes if a model with two degenerate levels[36] is used to calculate its values. The parameters of this model can be chosen in such a way that in this case, in agreement with experiment, χ_ν changes sign to the right of the middle of the shell.

For the example of the Sm isotopes one can see how the IBM describes the change in the properties of the nuclei in the case of the classical transition from an axial rotator to a spherical nucleus. Corresponding calculations of the states and $B(E2)$ ratios for ^{150}Sm, ^{152}Sm, and ^{152}Gd were made for the first time in the framework of the IBM-I in Ref. 37.

It follows from the data given in Ref. 37 that for the majority of the transitions the ratio of the probabilities differs little from the experimental value, although in some cases differences by 4–6 times are observed. The greatest discrepancy in the energy is about 200 keV at the level 2 MeV.

Figure 16a shows the energies of the excited states of the Sm isotopes in accordance with the calculations made in Ref. 35. It can be seen that the transition from the axial rotator to the spherical nucleus is described well, although there are some discrepancies between the experimental and calculated energies.

Figure 16b shows the optimal values of the parameters ε, k, χ_ν used in Ref. 35 to describe the structure of the Sm isotopes. We note especially that in the region in which there is essentially a phase transition from a static deformation to spherical nuclei the behavior of the parameters as functions of the number of neutrons differs little from the behavior of the parameters used in the description of any other family of isotopes.

The presence of a proton subshell filled at $Z = 64$, recently found in Ref. 38, has an important influence on the estimate of the number of proton bosons, which is an important parameter in the IBM. Thus, in the case of the $_{62}$Sm isotopes the number of proton bosons is 6 on the basis of the

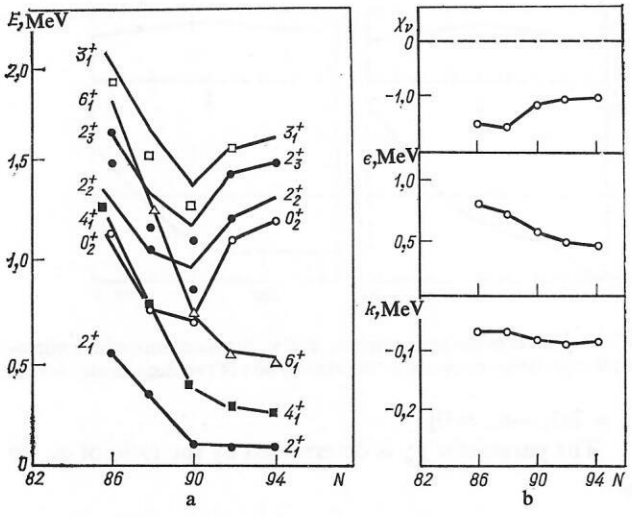

FIG. 16. Energies of excited states (a) and the parameters ε, k, and χ_ν ($\chi_\pi = -1.3$) (b) of Sm isotopes.

usual approach associated with an estimate of the number of valence particles or holes in the $Z = 50$–82 shell, whereas under the assumption of the existence of a subshell closed at $Z = 64$ with a sufficiently large energy gap separating it from the following levels the number of proton bosons is just one.

In Ref. 39, the behavior of this subshell is analyzed in its dependence on the number of neutrons in the nuclide. It is shown that as a result of the strong n–p interaction of the so-called spin-orbit partners (neutron and proton occupying the orbits $h_{9/2}$ and $h_{11/2}$) the filling with neutrons of the $h_{9/2}$ shell when $N \geqslant 88$ leads to transfer of an ever increasing number of protons to the $h_{11/2}$ orbit, and this also affects the development of the deformation, leading to the disappearance of the energy gap characteristic of the closed subshell with $Z = 64$.

The effect of the appearance and disappearance of the subshell in the framework of the IBM can be described approximately[40] if one determines the number n_π of active bosons at a neutron number $N < 88$ on the basis of the existence of a closed $Z = 50$–64 subshell, whereas for $N \geqslant 88$ one estimates n_π on the basis of a complete shell ($Z = 50$–82).

In Ref. 41, the validity of such an approach was tested on the basis of experimental data on the gyromagnetic values (g) of the 2_1^+ states of a number of nuclei in the region near $Z = 64$.

In the IBM-II, the M 1-transition operator has the form

$$\hat{T}(M1) = g_\pi \hat{L}_\pi + g_\nu \hat{L}_\nu, \tag{53}$$

where $g_{\pi,\nu}$ and $\hat{L}_{\pi,\nu}$ are the g factors and the angular-momentum operators for the proton and neutron bosons. Then the magnetic moment

$$\mu(2_1^+) = \left(\frac{8\pi}{15}\right)^{1/2} (g_\pi M_\pi + g_\nu M_\nu) \tag{54}$$

of the 2_1^+ state can be expressed in terms of the expectation values of the operators $\hat{L}_{\pi,\nu}$, i.e., in terms of $M_{\pi,\nu}$. Thus, between $\lambda(2_1^+)/M_\nu$ and M_π/M_ν there must be a linear dependence,

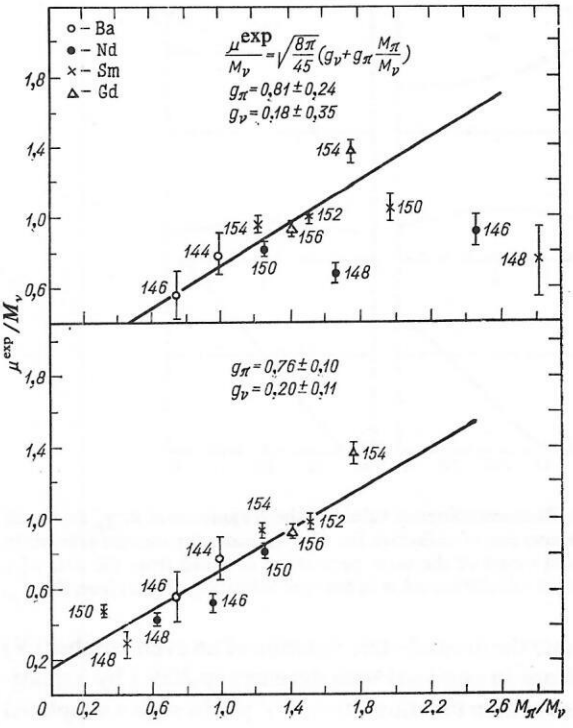

FIG. 17. Values of μ/M_ν as a function of the ratio M_π/M_ν of M 1-transition matrix elements. The values of M_π and M_ν are calculated under different assumptions about the existence of a $Z = 50$–64 proton subshell (see the text).

$$\mu(2_1^+)/M_\nu = \left(\frac{8\pi}{15}\right)^{1/2} (g_\nu + g_\pi M_\pi/M_\nu), \tag{55}$$

if we ignore the weak dependence of g_π and g_ν on the boson numbers n_π and n_ν.

Figure 17 shows $\lambda(2_1^+)/M_\nu$ as a function of M_π/M_ν for a number of Ba, Sm, Gd, and Nd isotopes. The straight lines are drawn by means of the least-squares method. The matrix elements M_π and M_ν were calculated in the framework of the IBM-II in the usual manner by optimizing the parameters of the Hamiltonian with respect to the energies of the excited states. In the calculations, the number n_π of proton bosons in the upper part of the figure was taken to be the value obtained from the assumption of a complete shell, while in the lower part it was obtained by assuming the existence of a subshell with $Z = 64$ for $N < 88$ and a complete $Z = 50$–82 shell for $N > 88$. The straight line in the upper part of the figure is fitted using only the points for which the n_π values were the same in both approaches. It can be seen from the figure that the points corresponding to nuclei with $N < 88$ do not lie on the straight line in the upper part of the figure. As follows from the lower part of the figure, the experimental data agree with the assumption of the existence of a closed shell with $Z = 64$ for $N < 88$. The experimental data confirm the linearity of the ratio $\lambda(2_1^+)/M_\nu$ and make it possible to determine the values of g_π and g_ν.

It should be noted that the approximation adopted in the calculation, which is equivalent to the assertion that the subshell with $Z = 64$ disappears abruptly when $N \geqslant 88$, is somewhat schematic, since it contradicts not only the quali-

tative description of the nature of the degradation of the shell associated with the interaction of spin-orbit parameters, and which to a certain degree presupposes a continuous nature of this process,[39] but also the microscopic calculations made in Ref. 42, in which it was shown that the effective number of proton bosons does not vanish, though it does have a minimum at $N = 64$. Nevertheless, the result shown in Fig. 17 illustrates well the fact that simple prescriptions for determining the number of bosons are not always automatically satisfied and there is a dependence of the effective number of bosons on the details of the shell states.

We should also mention Ref. 43, in which the results of measurements of $B(E2; 2_1^+ \to 0_1^+)$ for the isotopes $^{146}_{60}Nd_{86}$ and $^{148}_{62}Sm_{86}$ were compared with calculations in the IBM-II in which the choice of the number n_π of proton bosons is made under the usual assumption of a complete $Z = 50$–82 shell and under the assumption of the existence of a $Z = 50$–64 subshell. It is found that the experimental data agree better with the calculations when n_π is chosen on the basis of a complete shell. Since in this case the number of neutrons in each of the nuclides satisfies $N < 88$, in accordance with what we said above one would expect the opposite result. It is, however, possible that the unexpected result [the increase in the values of $B(E2; 2_1^+ \to 0_1^+)$ with increasing Z] is due to the fact that in the calculations for the two nuclei the effective charge is also taken to be the same ($e^* = 0.12e$·b).

6. TRANSITIONAL REGION OF THE Pt AND Os ISOTOPES

An analysis of the properties of the even isotopes of platinum (A = 190–194) was made for the first time in Ref. 44. It was established that the main features of the spectra up to excitation energies 2 MeV can be explained by means of the collective Hamiltonian (21) with $\varkappa_2 \ll \varkappa_1$. In addition, it was shown in Ref. 44 that the 0_2^+ state at the base of the β-vibrational band has seniority $v = 3$ and not $v = 0$, as predicted in Ref. 45. Such a situation is characteristic of the $O(6)$ limit of the IBM.

The Hamiltonian corresponding to the $O(6)$ limit was used in Ref. 46 to describe the ^{196}Pt nucleus. The calculations of Ref. 46 reproduce qualitatively the relative values of $B(E2)$ for numerous transitions from various levels, though the calculated energies differ in a number of cases strongly from the experimental values.

To describe the evolution of the properties of the Pt and Os isotopes with varying number of neutrons, Casten[47] diagonalized a simplified IBM-I Hamiltonian of the type $H = H[O(6)] - k\tilde{Q}\tilde{Q}$, where $\tilde{Q}\tilde{Q}$ describes the contribution of the quadrupole interaction that leads to the rotational spectrum [SU(3)]. Using a small number of parameters, Casten was able to correlate a large number of experimental data. Nevertheless, in this approach too the description of the energies remained unsatisfactory in a number of cases.

In Fig. 18, based on the data of Ref. 47, we show the $B(E2)$ values for some $E2$ transitions of the Os and Pt isotopes. The broken lines are the results of calculations in the framework of the IBM, and the chain lines the results of the calculations of Kumar and Baranger, hitherto regarded as the best.

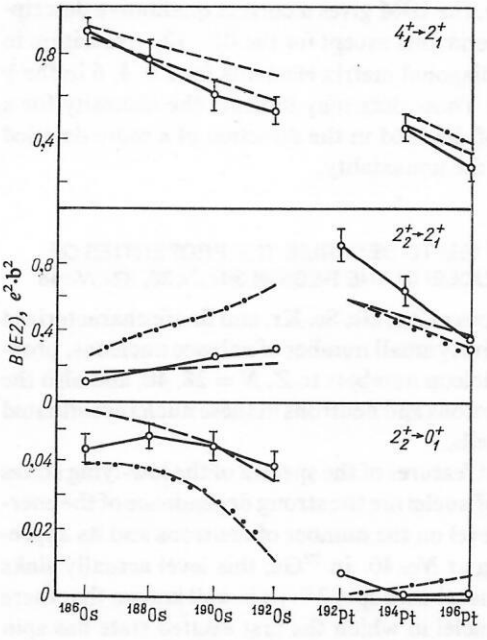

FIG. 18. Absolute probabilities of the $E2$ transitions $4_1^+ \to 2_1^+, 2_2^+ \to 2_1^+$, $2_2^+ \to 0_1^+$ of Os and Pt isotopes in accordance with the data of Ref. 47. The continuous line represents the experiment, the broken line the interacting-boson model, and the chain line the calculations of Kumar and Baranger.

Calculations of the properties of Os and Pt isotopes have also been made on the basis of diagonalization of the complete IBM-II Hamiltonian.[48] The results for the relative probabilities of the $E2$ transitions differ little from those obtained using the simplified IBM-I Hamiltonian, but the description of the energies of the excited states is much improved. This follows from Fig. 19, which shows the calculated and experimental energies of the levels of the Os isotopes.

In his review,[49] Stephens compares the experimental data on the probabilities of $E2$ transitions and the quadrupole moments of the levels in ^{194}Pt, ^{190}Os, and ^{192}Os with the predictions of various models: rigid asymmetric rotator, γ-unstable or γ-soft rotator, the boson expansion theory (BET),[50] and the IBM-II with the parameters found in Ref. 48. The results of these comparisons show that none of the models considered is completely adequate in explaining the

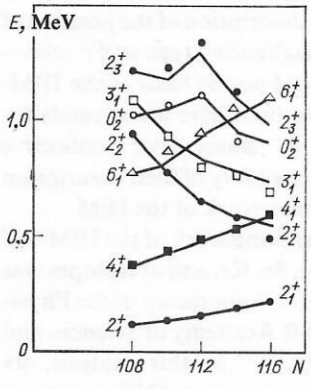

FIG. 19. Excitation energies of states of Os isotopes in accordance with the data of Ref. 48.

data. Basically, the IBM gives a correct qualitative description of the experiments except for the $0_2^+ \to 2_2^+$ transition in ^{194}Pt and the diagonal matrix elements for $I = 4, 6$ in the γ band of ^{192}Os. These data may indicate the necessity for a modification of the IBM in the direction of a more detailed description of the nonaxiality.

7. USE OF THE IBM TO DESCRIBE THE PROPERTIES OF EVEN-EVEN NUCLEI IN THE REGION $30 \leqslant Z \leqslant 38$, $32 \leqslant N \leqslant 48$

The isotopes of Zn, Ge, Se, Kr, and Sr are characterized by a comparatively small number of valence nucleons, proximity of the nucleon numbers to $Z, N = 28, 40$, and also the fact that the protons and neutrons in these nuclei are situated in the same shells.

Important features of the spectra of the low-lying states of this region of nuclei are the strong dependence of the energy of the 0_2^+ level on the number of neutrons and its appreciable lowering at $N \simeq 40$. In ^{72}Ge, this level actually sinks below the first level with spin 2^+. (It is well known that there exist several nuclei in which the first excited state has spin 0^+: ^{16}O, ^{40}Ca, ^{72}Ge, ^{90}Zr, ^{96}Zr, ^{98}Zr, ^{98}Mo.)

The IBM (in the variant IBM-II) was applied to the Kr isotopes for the first time in Ref. 51. To simplify the analysis, a linear dependence of χ_ν on the number of neutrons was assumed (see Ref. 52). The energies of the 0_2^+ levels calculated in Ref. 51 were found to be about 0.5 MeV above the observed energies. This suggested to the authors of Ref. 51 that the 0_2^+ state has a noncollective nature. Similar conclusions about the nature of the 0_2^+ states in the Ge isotopes were reached even earlier by the authors of Ref. 52, who made calculations in the framework of the theory of boson expansions. It was concluded in Ref. 52 that neutron pairing vibrations make an important contribution to the 0_2^+ states.

There are, however, arguments against such an interpretation of the low-lying 0_2^+ states in this region of nuclei. First, the probabilities of $E2$ transitions from the 0_2^+ levels could not be reproduced in the calculations of Ref. 52. Second, Kumar's calculations[53] of the structure of the states of the Ge isotopes in terms of Bohr's collective β and γ variables using the dynamic deformation model (DDM) to calculate the parameters of the collective Hamiltonian gave a very reasonable explanation of the anomalously low position of the 0_2^+ level in ^{72}Ge and the large $B(E2; 0_2^+ \to 2_2^+)$ values. Third and finally, a satisfactory description of the position of the low-lying 0_2^+ levels in the neighboring region of nuclei—in the Mo isotopes—was achieved on the basis of the IBM-I.[54,55] All these arguments show that there are grounds for adhering to the view that the 0_2^+ states have a collective nature and for considering the possibility of their description along with other states in the framework of the IBM.

A systematic analysis in the framework of the IBM-I of the properties of the even Zn, Ge, Se, Kr, and Sr isotopes was made by members of the Cyclotron Laboratory of the Physicotechnical Institute of the USSR Academy of Sciences and the Leningrad State University.[56–60] In this analysis, six IBM-I parameters [$\varepsilon, \varkappa_1, \varkappa_2, c_0, c_2, c_4$; see (21)] were basically determined from the energies of the lowest six levels $2_1^+, 4_1^+, 6_1^+, 0_2^+, 2_2^+, 4_2^+$. The calculations of $B(E2)$ used the parameter χ_{E2}, which, as was established in Refs. 56–60, is fairly close to the parameter $\chi = \varkappa_1/2\varkappa_1$ [see (24)]. The parameter e^*, which has the nature of a scale factor, was determined from $B(E2; 2_1^+ \to 0_1^+)$. Although in the investigated isotopes the number of low-lying levels usually does not exceed 12, the total number of experimental data [values of the level energies and $B(E2)$] exceeds, as a rule, the number of parameters by 3–4 times.

The energies of the levels included in the procedure for determining the parameters are reproduced in the calculations with an error $\lesssim 50$ keV. For the remaining levels, the largest, and rather systematic, discrepancy occurs for levels with odd spins. However, it should be noted that the not entirely successful description of, for example, the 3_1^+ levels in Ge is characteristic of many collective models; they all give values somewhat too large. This may indicate that in these states certain additional degrees of freedom are manifested. It is possible that the doubling in the number of degrees of freedom in the IBM-II (proton and neutron bosons) is manifested in the somewhat better description of the 3_1^+ levels in the Se and Kr isotopes in the IBM-II framework.[61–63]

We should also mention the general tendency for the calculated energies of levels with spins $\gtrsim 8$ to exceed the experimental values systematically.

The results of the analysis of the energy levels, the reduced probabilities of $E2$ transitions, and $Q(2_1^+)$ in the framework of the IBM-I for the Zn isotopes are given in Fig. 20 and in Table II. Overall, the model correctly reproduces the behavior of the energies of the excited states and the values of $B(E2)$ and $Q(2_1^+)$ (in ^{64}Zn and ^{70}Zn), although there are individual significant discrepancies in the values of $B(E2)$, for example, $B(E2)$: $0_2^+ \to 2_1^+$ in ^{64}Zn.[56]

It should be noted that the IBM and other collective models encounter difficulties in the description of the quadrupole transitions from the levels 0_2^+ and 2_2^+ or to them, and also in the description of the quadrupole moments in the Ge isotopes. In the IBM-I calculations made in Refs. 57, 58, and 60 for Ge isotopes, these probabilities are basically close to the experimental values, but the calculated values of $Q(2_1^+)$ in ^{70,72}Ge are not correct. It is interesting to note that the results of Refs. 57, 58, and 60 are close to Kumar's results (Table III, DDM column). Structures of the Ge isotopes were also calculated in Ref. 64 on the basis of a more complicated variant of the IBM-II, which takes into account the interaction of two configurations. A more detailed exposition of this paper and a comparison of it with the data of Refs. 57, 58, and 60 will be given below (see Sec. 10).

In Fig. 21, the calculated energies of the excited states of the Se isotopes are compared with the experimental values. The same figure shows the positions of the 0_2^+ levels calculated in the IBM-II in Ref. 51. It can be seen from Fig. 21 that these values differ appreciably from the experimental ones. The theoretical values of the remaining levels in the interval to 2.5–3.0 MeV calculated in the IBM-I (Refs. 56, 59, 60, and 65) and in the IBM-II (Refs. 61 and 62) are virtually identical.

In Table IV, we give the results of calculations of the values of $B(E2)$ and $Q(2_1^+)$ for Se with $A = 72$–78.[56] Com-

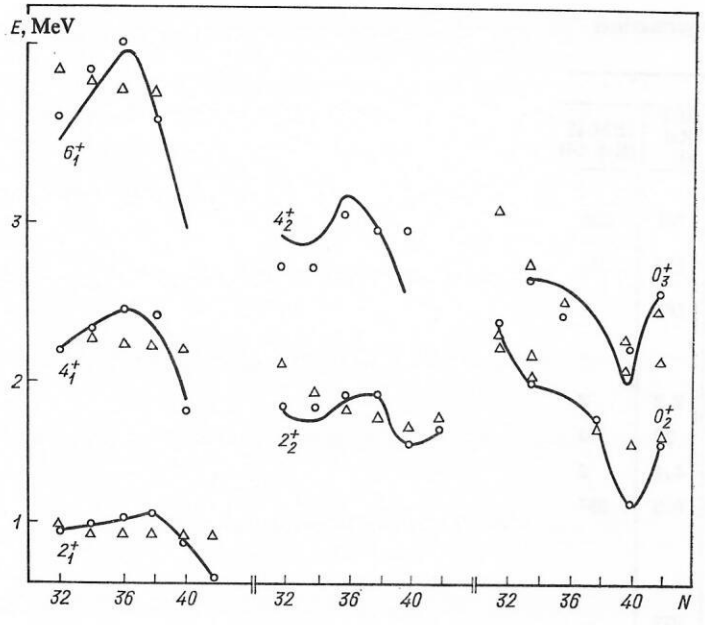

FIG. 20. Calculated and experimental energies of excited states of the isotopes $^{62-72}$Zn. The continuous curves represent the IBM-I calculation, the open circles the experiment, and the open triangles the IBM-II calculation.[28]

parison of them with the experiments show that overall the IBM predictions agree with the experiments for all the Se isotopes, though in the case of small $B(E2)$ values the discrepancies may be by a few times. For the light Se isotopes, the $B(E2)$ values are not described with complete success along the yrast band, though variation of the parameter χ_{E2} makes it possible to improve somewhat the description of these $B(E2)$ values (the calculations of Table IV are made for a fixed value of $\chi_{E2} = \varkappa_2/2\varkappa_1$).

The description of the spectra and probabilities of $E2$ transitions in the Kr isotopes was successful (Fig. 22 and Table V, which are taken from Ref. 60). It does not follow from these calculations that the 0_2^+ states in the Kr isotopes have some particular, noncollective nature, as was asserted in Ref. 51. It should, however, be mentioned that in the krypton isotopes there are no experimental $B(E2; 0_2^+ \to 2_1^+)$ values, but these are very important for clarifying the structure of these states.

In the Sr isotopes, the experimental material on the $B(E2)$ values is very sparse, so that for these isotopes we give only the calculations of the energy spectrum (Fig. 23). The properties of the Sr isotopes were also calculated in the framework of the IBM in Ref. 66.

TABLE II. Experimental and theoretical (IBM-I) values of $B(E2)$ and $Q(2_1^+)$ in zinc isotopes.*

transition $I_i I_f$	$A=62$		$A=64$		$A=66$		$A=68$	
	experiment	calculation	Experiment	calculation	Experiment	calculation	experiment	calculation
$2_1\,0_1$	241 ± 14	241	316 ± 10	316	274 ± 10	274	272 ± 12	272
$4_1\,2_1$	360^{+130}_{-115}	287	461 ± 140	414	130	387	—	—
$6_1\,4_1$	275^{+100}_{-115}	197	321 ± 70	358	178	394	—	—
$0_2\,2_1$	—	—	$0{,}86\pm0{,}05$	37	—	0,46	—	373
$0_2\,2_2$	—	—	935 ± 120	356	—	395	750 ± 150	385
$2_2\,2_1$	260 ± 50	254	560 ± 60	359	1700^{+400}_{-700}	387	270 ± 50	304
$2_2\,0_1$	$4{,}8^{+8}_{-6}$	2,3	$3{,}5\pm0{,}3$	4,3	$0{,}76\pm0{,}12$	3,9	$8{,}9\pm1{,}6$	7,8
$0_3\,2_1$	—	—	140 ± 42	123	—	—	—	—
$0_3\,2_2$	—	—	$20-85$ $22{,}90$	12	—	—	—	—
$4_2\,2_2$	120^{+16}_{-9}	101	545 ± 125	183	—	—	—	—
$4_2\,4_1$	260^{+70}_{-60}	77	152^{+180}_{-83}	135	—	—	—	—
$Q(2_1^+)$	—	$-10{,}9$	-13.5	$-13{,}9$	—	$-0{,}08$	—	$-22{,}4$

*In Tables II–V, $B(E2)$ is measured in single-particle units, and Q in $e\cdot F^2$.

TABLE III. Experimental and theoretical values of $B(E2)$ and $Q(2_1^+)$ in germanium isotopes.

Transition $I_i I_f$	$A=68$				$A=70$				
	experiment	IBM-I	BET (Ref. 52)	IBM-II (Ref. 64)	experiment	IBM-I	DDM (Ref. 53)	BET (Ref. 52)	IBM-II (Ref. 64)
$2_1\,0_1$	247±82	245	257	183	357^{+130}_{-70}	357	460	361	238
$4_1\,2_1$	330±80	362	387	272	437^{+250}_{-120}	610	—	523	354
$6_1\,4_1$	280±70	367	430	—	640^{+290}_{-150}	678	—	567	—
$8_1\,6_1$	—	—	—	—	720^{+360}_{-240}	558	—	—	—
$2_2\,0_1$	3,3	5,5	3,3	1,4	16^{+10}_{-8}	37	32	2,2	2
$0_2\,2_1$	—	146	203	74	600±150	758	680	26	70
$2_2\,0_2$	—	47	22	0,5	425^{+250}_{-200}	214	280	4,4	2
$2_2\,2_1$	230±50	291	376	262	500±190	215	—	509	357
$4_1\,2_2$	—	—	—	—	307^{+175}_{-82}	110	—	—	—
$4_2\,2_2$	—	—	—	—	500^{+250}_{-130}	257	—	—	—
$4_2\,4_1$	—	—	—	—	750	29	—	273	—
$3_1\,2_2$	~ 50	256	319	—	20^{+8}_{-5}	122	—	411	—
$3_1\,2_1$	~ 0,33	4,2	—	—	—	—	—	--	—
$2_3\,0_1$	—	—	—	—	$0{,}8^{+0{,}3}_{-0{,}2}$	0,3	—	—	—
$2_3\,0_2$	—	—	—	—	180^{+80}_{-40}	60	—	—	—
$6_2\,4_2$	—	—	—	—	470^{+200}_{-110}	172	—	—	—
$Q(2_1^+)$	—	−15,6	−11	−0,4	3±6 9±6	−33	15	−11,5	−1,8

Transition $I_i I_f$	$A=72$				
	Experiment	IBM-I	DDM (Ref. 53)	BET (Ref. 52)	IBM-II (Ref. 64)
$2_1\,0_1$	421±10	418	540	440	418
$4_1\,2_1$	840±90	1058	—	636	618
$6_1\,4_1$	660±200	1155	—	687	—
$8_1\,6_1$	700±300	1016	—	—	—
$10_1\,8_1$	820±400	801	—	—	—
$12_1\,10_1$	480±300	550	—	—	—
$2_1\,0_1$	4,6±2,0	3,7	—	—	9
$2_2\,2_1$	140 1440	86	440	675	597
$0_2\,2_1$	2050 1300	2090	810	—	310
$0_2\,2_2$	5±2	3,3	—	—	65
$3_1\,2_1$	$3\cdot10^{-2}$	1,5	—	—	—
$Q(2_1^+)$	−13±6 −5±6	−56	23	−0,2	−8,2

Transition $I_i I_f$	$A=74$					$A=76$			
	Experiment	IBM-I	DDM (Ref. 53)	BET (Ref. 52)	IBM-II (Ref. 64)	experiment	IBM-I	BET (Ref. 52)	IBM-II (Ref. 64)
$2_1\,0_1$	609±6	609	660	594	730	556±6	556	600	605
$4_1\,2_1$	667±64	858	--	897	1048	730±130	727	891	816
$2_2\,0_1$	13±5	11	50	3	22	17±3	11,7	16	14
$0_2\,2_1$	400	198	—	394	120	—	9,9	267	--
$2_2\,2_1$	1000±200	661	—	798	697	740±90	703	520	792
$Q(2_1^+)$	−25±6	−24,8	24	−18	−24,4	−12±6 −3±6	−8,8	−34	−21

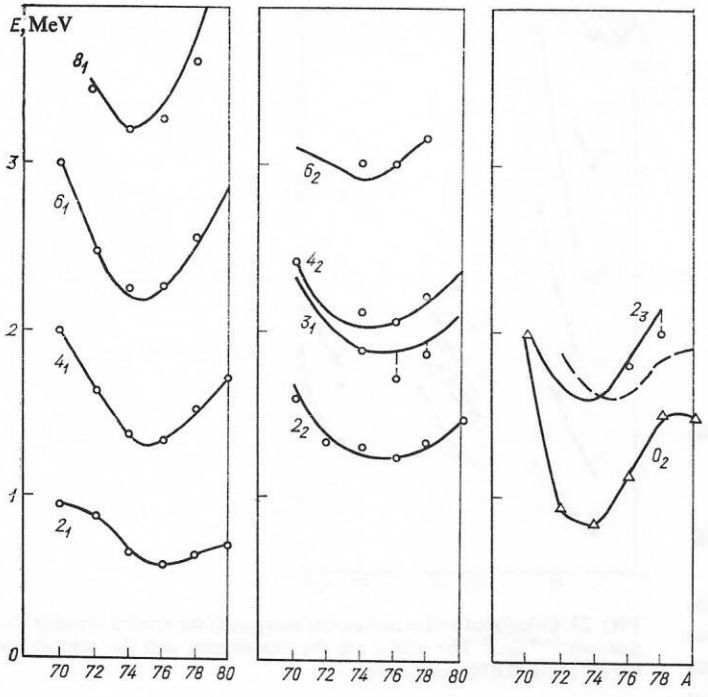

FIG. 21. Calculated and experimental energies of excited states of the isotopes $^{70-80}$Se.

TABLE IV. Experimental and theoretical (IBM-I) values of $B(E2)$ and $Q(2_1^+)$ in selenium isotopes.

transition $I_i I_j$	$A=72$		$A=74$		$A=76$		$A=78$	
	Experiment	calculation	Experiment	calculation	Experiment	calculation	Experiment	calculation
$2_1\,0_1$	19 ± 2	19,1	40,1	40	44 ± 1	44	39 ± 3	39
$4_1\,2_1$	53^{+8}_{-6}	31	80 ± 3	82	72 ± 21	69	57 ± 13	57
$6_1\,4_1$	61^{+12}_{-9}	38	45 ± 11	104	77 ± 10	77	47 ± 14	61
$8_1\,6_1$	71^{+16}_{-11}	29	53 ± 4	107	88^{+58}_{-23}	74	57 ± 19	55
$10_1\,8_1$	95^{+25}_{-17}	22	48 ± 7	96	53 ± 10	63	49	42
$12_1\,10_1$	90^{+22}_{-15}	15	47 ± 60	79	77^{+77}_{-60}	46	25	24
$0_2\,2_1$	—	48	73 ± 22	109	—	37	29	21
$2_2\,2_1$	—	—	—	—	44 ± 2	37	24 ± 8	44
$2_2\,0_1$	$0{,}40\pm0{,}06$	2,7	$0{,}98\pm0{,}27$	2,9	$1{,}25\pm0{,}05$	1,5	$0{,}8\pm0{,}2$	0,7
$3_1\,2_1$	—	—	—	—	$2{,}4^{+1{,}1}_{-1{,}3}$	1,7	1,6—4,7	0,8
$3_1\,2_2$	—	—	—	—	81^{+36}_{-43}	45	5	41
$4_2\,2_2$	—	—	$14{,}1^{+6{,}5}_{-4{,}3}$	50	32^{+24}_{-10}	36	55 ± 23	30
$4_2\,2_1$	—	—	$0{,}49^{+0{,}27}_{-0{,}11}$	3,1	$0{,}05\pm0{,}01$	0,66	$0{,}25\pm0{,}12$	0,27
$4_2\,4_1$	—	—	—	—	9	18	36 ± 6	22
$5_1\,3_1$	—	—	42 ± 18	45	70^{+22}_{-19}	36	66 ± 23	28
$5_1\,4_1$	—	—	—	—	$0{,}8^{+0{,}5}_{-0{,}3}$	0,9	$2{,}0\pm1{,}0$ 58^{+22}_{-13}	0,4
$6_2\,4_2$	—	—	—	64	31 ± 11	48	87^{+45}_{-25}	37
$6_2\,4_1$	—	—	$1{,}8\pm0{,}8$	2,6	—	0,4	$0{,}4^{+0{,}5}_{-0{,}3}$	0,60
$7_1\,5_1$	—	—	27 ± 1	58	40^{+15}_{-13}	42	29 ± 8	29
$9_1\,7_1$	—	—	36 ± 2	54	38^{+11}_{-8}	35	9 ± 3	18
$Q(2_1^+)$			-36 ± 7	-60	-31 ± 4 -34 ± 7 -44 ± 9	-44	-28 ± 5 -26 ± 9 -40 ± 8	-28

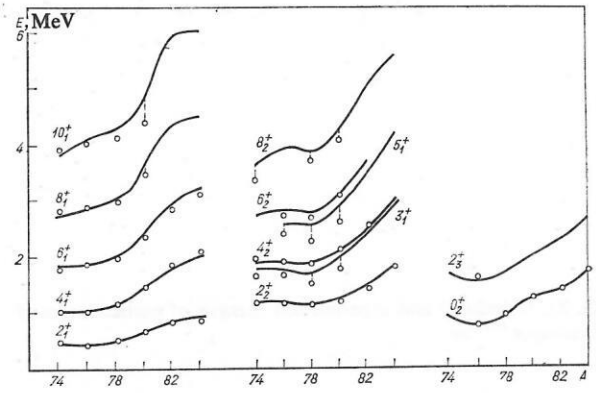

FIG. 22. Calculated and experimental energies of excited states of the isotopes $^{74-84}$Kr.

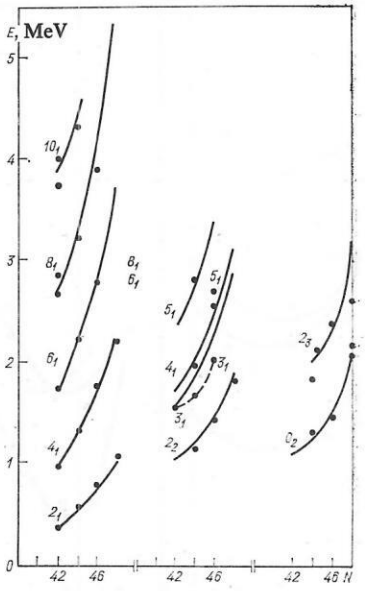

FIG. 23. Calculated and experimental energies of the excited states of the isotopes $^{80-86}$Sr.[56] The points are the experiment, and the continuous curves are the IBM-I calculation.

8. ESTIMATES OF THE DEFORMATIONS OF NUCLEI ON THE BASIS OF THE IBM

The interacting-boson model has several possibilities for estimating deformations. The first conclusions about the deformation of various states in one and the same nucleus (^{150}Sm, ^{152}Gd) were obtained in Ref. 37 on the basis of an analysis of boson wave functions. This method was developed in Refs. 59 and 60, in which calculations were made of the overlap integrals of the wave functions corresponding to the SU(5), SU(3), and $O(6)$ limits of the IBM with the functions $\psi(L)$ obtained by exact diagonalization of the IBM-I Hamiltonian with parameters that make it possible to describe the real spectrum.

As was shown, for example, in Refs. 20 and 24, the SU(5) limit corresponds to a minimum of the energy at $\tilde{\beta}=0$ ($\tilde{\beta}$ is the deformation parameter in the IBM); in the SU(3) limit, a minimum of the energy is attained for axisymmetric deformation $\tilde{\beta}\simeq\sqrt{2}$, and in the $O(6)$ limit the energy does not depend on γ and attains its minimum at $\tilde{\beta}\simeq 1$. The quantity $\tilde{\beta}$ is related to the usual shape deformation parameter by the approximate relation $\beta\simeq 2n\tilde{\beta}/A$, where A is the mass number and n is the number of bosons.[20] When the integral of the overlap of $\Psi(L)$ with a function of some limit is maximal (say, of order 0.8 or greater), it can be concluded that the deformation in this state can be characterized by the parameter $\tilde{\beta}$ given by the corresponding limit of the IBM. But if two or three integrals are comparable in magnitude, this means that in the given state the nucleus is either soft or has some intermediate shape.

In a consideration of overlap integrals, it must be borne in mind that the functions of the three limiting cases are not mutually orthogonal, and their overlapping increases with increasing L, so that for $L=2n$ all three functions are the same. For $L\ll 2n$, their mutual overlapping is comparatively small (Table VI).

In Table VII, we give the integrals of the overlapping of the yrast-band state functions of the Se isotopes with the yrast-band functions of the analytic limits of the IBM, i.e.,

TABLE V. Comparison of experimental values of $B(E2)$ with the values calculated in the framework of the IBM-I for krypton isotopes.

I_iI_j	$A=76$		$A=78$		$A=80$	
	Experiment	calculation	Experiment	calculation	Experiment	calculation
$2_1\,0_1$	59±7	59	64±5	64	37±3	37
$4_1\,2_1$	76±25	114	86±12	103	44±9	58
$6_1\,4_1$	89±8	141	89±14	119	50±20	67
$8_1\,6_1$	129±13	153	105±29	122	88±55	66
$10_1\,8_1$	129±19	152	102±40	114	46±23	58
$12_1\,10_1$	—	—	95±50	97	84±50	44
$14_1\,12_1$	—	—	59±25	72	16	25
$2_2\,2_1$	—	—	34	52	24±6	49
$2_2\,0_1$	—	—	1,21±0,20	1,9	0,28±0,7	0,32
$3_1\,2_1$	—	—	3,1±0,3	2,9	0,58±0,11	0,44
$3_1\,2_2$	—	—	77±17	68	35±6	44
$4_2\,2_2$	47±16	60	63±17	54	48±20	33
$4_2\,2_1$	0,6±0,2	0,6	0,3±0,2	0,4	0,2	0,1
$4_2\,4_1$	27±8	9	44	28	32±15	26
$5_1\,3_1$	101±19	56	119±60	58	50±20	34
$5_1\,4_1$	3,4±0,7	1,9	4,2	1,5	1,2±0,4	0,3
$6_2\,4_2$	—	—	44±29	77	35±17	44
$7_1\,5_1$	79±32	82	76±32	73	35	39

TABLE VI. Squares of the integrals of the mutual overlapping of the wave functions of the SU(5), SU(3), and $O(6)$ analytic limits of the IBM for states of the $n = 8$ yrast band.

I	$\lvert\langle SU(3) \mid SU(5)\rangle\rvert^2$	$\lvert\langle O(6) \mid SU(5)\rangle\rvert^2$	I	$\lvert\langle SU(3) \mid SU(5)\rangle\rvert^2$	$\lvert\langle O(6) \mid SU(5)\rangle\rvert^2$
0	0,0026	0,072	10	0,27	0,83
2	0,0098	0,17	12	0,45	0,95
4	0,030	0,32	14	0,69	1,0
6	0,071	0,50	16	1,0	1,0
8	0,15	0,68			

SU(5), SU(3), and $O(6)$. The overlappings of the functions of the 0_2^+ states were calculated with the two-boson SU(5) configuration with the function $(\lambda, \lambda) = (2n, 0)$ and $L = 0$ in SU(3) and the 0_2^+ state in $O(6)$.[58]

Besides the calculation of the overlap integrals, to elucidate the question of nuclear deformation one can consider the expectation value with respect to H of some intrinsic state function[20,24]:

$$\Psi \sim \left\{s^+ + \tilde{\beta}\left[d_0^+ \cos\gamma + (d_2^+ + d_{-2}^+)\ \frac{1}{\sqrt{2}} \sin\gamma\right]\right\}^n \mid 0). \quad (56)$$

In the boson description, this function plays the same part as the nucleon function of the intrinsic state (referred to a coordinate system attached to the nucleus) in the theory of deformed nuclei:

$$\rangle = \frac{\langle\Psi \mid H \mid \Psi\rangle}{\langle\Psi \mid \Psi\rangle} = \frac{n\tilde{\beta}^2}{(1+\tilde{\beta}^2)^2}\left\{\varepsilon + 2\varkappa_1 (n-1)\right.$$
$$- \sqrt{\frac{8}{7}}\,\varkappa_2 (n-1)\,\tilde{\beta}\cos 3\gamma$$
$$\left. + \left[\left(\frac{c_0}{10} + \frac{c_2}{7} + \frac{9c_4}{35}\right)(n-1) + \varepsilon\right]\tilde{\beta}^2\right\}, \quad (57)$$

where $\varepsilon, \varkappa_1, \varkappa_2, c_0, c_2, c_4$ are the parameters of the Hamiltonian (21). It can be seen from (6) that $\langle H\rangle$ has a minimum only for $\gamma = 0$ or $\gamma = \pi/3$, depending on the sign of $\varkappa_2$ ($\varkappa_2 > 0$, $\gamma = 0$; $\varkappa_2 < 0$, $\gamma = \pi/3$). In this sense, one says that nonaxial deformations are impossible in the IBM. The results of calculations of the dependence of $\langle H\rangle$ on $\tilde{\beta}$ for $\gamma = 0$ and $\gamma = \pi/3$ (in all the calculations, $\varkappa_2 > 0$) are shown in Fig. 24 for the Se isotopes.

It is interesting to compare the $\langle H\rangle$ data in Fig. 24 with the data in Table VII, which contains the overlap integrals. It can be seen from Fig. 24 that the Se isotopes with A equal to 70, 72, 74 have the equilibrium value $\tilde{\beta} = 0$, and the maximal overlapping is with the SU(5) ground state (see Table VII). According to the data of Ref. 59, the isotopes ^{78}Se and ^{80}Se are soft with respect to $\tilde{\beta}$ and γ-unstable. The degree of softness with respect to $\tilde{\beta}$ can be defined as $S = \partial^2\langle H\rangle/\partial\tilde{\beta}^2$, where $\langle H\rangle$ is given by (57). With increasing number of neutrons, there is an increase in S. Thus, for the isotopes ^{72}Se, ^{76}Se, and ^{80}Se the values of S are 0.09, 0.44, and 0.62.[59] It should be noted that for the heavy Se isotopes a small change in the parameters of the IBM Hamiltonian can, without destroying the agreement between the theory and experiment, result in the minimun of $\langle H\rangle$ (57) being attained at $\tilde{\beta} \neq 0$. Thus, for nuclei sufficiently soft with respect to $\tilde{\beta}$ the IBM cannot give unambiguous indications about the degree of their deformation.

We also draw attention to a characteristic feature of the variation of the overlap integrals along the yrast band. As follows from Table VII, there is a gradual increase in the overlapping with the SU(3) and $O(6)$ functions, i.e., as they unwind, the nuclei become more and more deformed. (At angular momenta greater than 6 or 8, this conclusion may be appreciably changed when allowance is made for bosons with angular momentum 4 or quasiparticle pairs with large angular momenta.)

The calculations made in Refs. 59 and 60 show that the 0_2^+ states in the Ge, Se, and Kr isotopes have a fairly complicated nature, so that the two-phonon component [SU(5) limit] is small. The clearest examples in this sense are the isotopes ^{70}Ge, ^{72}Ge and ^{72}Se, ^{74}Se. In these cases, the overlapping of $\Psi(0_2^+)$ with the SU(3)-limit function $(\lambda, \lambda) = (2n, 0)$ dominates over the other integrals. Since the ground states of these isotopes are spherical, for the given isotopes one can speak of a coexistence of shapes: sphericity in the ground state and axial deformation in the 0_2^+ state (see Table VII).

Quantitative conclusions about the increase of the deformation in the 0_2^+ state compared with the 0_1^+ state can be

TABLE VII. Squares of the integrals of the overlapping of the wave functions of the yrast band and O_2^+ states of Se isotopes with the functions of the analytic limits of the IBM (n is the number of bosons).

State	$A = 72$, $n = 8$			$A = 74$, $n = 8$			$A = 76$, $n = 7$			$A = 78$, $n = 6$			$A = 80$, $n = 5$		
	$SU(5)$	$O(6)$	$SU(3)$	$SU(5)$	$O(6)$	$SU(3)$	$SU(5)$	$O(6)$	$SU(3)$	$SU(5)$	$O(6)$	$SU(3)$	$SU(5)$	$O(6)$	$SU(3)$
0_1	0,79	0,40	0,10	0,79	0,34	0,09	0,63	0,63	0,22	0,51	0,85	0,42	0,36	0,98	0,67
0_2	0,08	0,26	0,77	0,14	0,36	0,69	0,26	0,29	0,58	0,51	0,69	0,49	0,38	0,56	0,25
2_1	0,48	0,70	0,50	0,54	0,58	0,36	0,57	0,74	0,40	0,52	0,60	0,85	0,36	0,90	0,75
4_1	0,14	0,50	0,84	0,36	0,59	0,66	0,56	0,77	0,58	0,54	0,83	0,76	0,46	0,87	0,82
6_1	0,07	0,31	0,81	0,29	0,53	0,87	0,58	0,78	0,73	0,59	0,79	0,86	0,42	0,70	0,69
8_1	0,04	0,23	0,60	0,26	0,46	0,97	0,64	0,78	0,84	0,64	0,74	0,96			

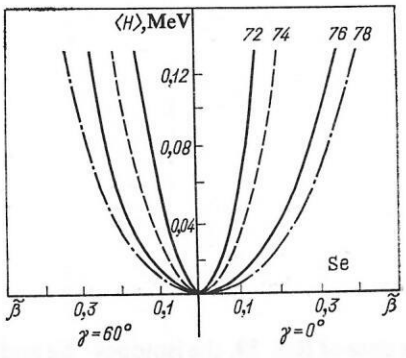

FIG. 24. Dependence of $\langle H \rangle$ on $\tilde{\beta}$ for the isotopes ^{70,72,74}Se.

obtained by calculating the value of R:

$$R=\frac{\langle 0_2^+ \mid QQ \mid 0_2^+\rangle}{\langle 0_1^+ \mid QQ \mid 0_1^+\rangle}=\frac{\sum_i B(E2;\ 2_i^+ \to 0_2^+)}{\sum_k B(E2;\ 2_k^+ \to 0_1^+)}=\frac{\beta^2(0_2^+)}{\beta^2(0_1^+)}. \qquad (58)$$

In Ref. 67, it was proposed that R should be regarded as a measure of the ratio of the mean-square deformations. It can be seen from the data in Table VIII that in the Ge, Se, and Kr isotopes with the number of neutrons N equal to 38 and 40 values $R \gtrsim 1.2$ are observed. As was noted earlier, in Se with N equal to 38 or 40 this conclusion follows directly from an analysis of the values of the overlap integrals. In the case of the Kr isotopes with N equal to 38 or 40, analysis of the overlap integrals indicates only that the wave function of the 0_2^+ state has a complicated nature and is "unlike" any function of the analytic limits.

Thus, the results of the calculations given above confirm the qualitative conclusions drawn earlier[68] to the effect that states with different deformations exist in the Ge and Se isotopes.

There is a different situation in the ^{74}Kr and ^{76}Kr isotopes. Investigating the properties of these nuclei, the authors of Ref. 69 concluded that the ground states of ^{74}Kr and ^{76}Kr are strongly deformed, while the 0_2^+ states are spherical. Assuming repulsion of the 0_1^+ and 0_2^+ states in these isotopes as a result of their interaction, they calculated[69] the "unperturbed" value of $E(2_1^+)$–$E(0_1^+)$ and found it to be very small (200 keV in ^{74}Kr and 237 keV in ^{76}Kr). This fact served as their main argument for the existence of a strong deformation of the Kr isotopes. However, calculations of the overlap integrals, the values of $\langle H \rangle$ as functions of $\tilde{\beta}$, and also R (58) made in Ref. 60 on the basis of the IBM show that the shape of the $^{74-78}$Kr nuclei in the 0_2^+ states cannot be less deformed than in the ground state.

To conclude this section, we note that the analysis of the structure of the various isotopes on the basis of a comparison of their deformations serves only as a clarifying interpretation of the properties of these states. To make calculations of the energies, transition probabilities, and static moments in the IBM, there is no need to ascribe definite deformations to the investigated states.

9. MIXING OF CONFIGURATIONS WITH DIFFERENT NUMBERS OF BOSONS AND ITS INFLUENCE ON THE EFFECT OF THE CUTOFF WITH RESPECT TO THE NUMBER OF BOSONS

We now consider some modifications of the IBM that have been proposed for extending the number of degrees of freedom used in the model. The various modifications at present have one common feature—besides the five quadrupole degrees of freedom (and the scalar degree of freedom, if the Arima-Iachello formulation[15] is used), they all include certain new degrees of freedom: additional quadrupole (d') and scalar (s') bosons, hexadecapole (g) bosons with spin 4, and two-quasiparticle excitations with large angular momenta. The assumption of the existence in one nucleus of different boson configurations (with different total numbers of s and d bosons or different types of proton bosons) is also associated with the need to extend the number of degrees of freedom. Allowance for these additional degrees of freedom enriches the theoretical spectrum with new states and makes the theory more flexible in the description of the experimental data. In principle, the admissibility of these extensions of the model is not in doubt, since at energies $\gtrsim 2\Delta$ (Δ is the gap parameter) there is a fairly large number of weakly collectivized (mainly two-quasiparticle) states that interact with the collective states. However, the phenomenological introduction of the interaction of the additional bosons with the collective bosons or the interaction of different configurations increases the number of variable parameters, and this to a certain degree diminishes the value of such constructions.

The excitation of proton or neutron pairs through a closed shell leads to effects that are frequently referred to as coexistence of shapes. Well known in this respect are the examples with different behaviors of the lower and excited states of the ^{16}O and ^{40}Ca nuclei. Comparatively recently,[70] an investigation of the (^{3}He, n) reaction revealed strong population of low-lying 0^+ states of tin isotopes which were found to be the bases of bands that recall rotational bands in their properties.[71] Duval and Barrett[72] proposed a method of describing these coexisting collective structures in the framework of the IBM-II and used it to describe the proper-

TABLE VIII. Values of $R=\beta^2(0_2^+)/\beta^2(0_1^+)$ for Ge, Se, and Kr isotopes.

Isotopes	Ge			Se				Kr				
A	70	72	74	72	74	76	78	74	76	78	80	82
R	1,22	1,39	0,73	1,25	1,56	0,92	0,74	1,27	1,43	1,00	0,97	0,87

ties of the mercury isotopes. Besides the configuration generally used in the IBM-II, in which the numbers of proton and neutron bosons (n_π and n_ν) are determined by the numbers of valence protons and neutrons or their holes (for the mercury isotopes, $n_\pi = 1$), they also introduce a configuration with $n_\pi = 3$, which corresponds to the transfer of one pair of protons through a shell and the appearance of one further pair of proton holes in shell states situated below $Z = 82$. The eigenstates of each of the configurations are calculated separately using the IBM-II Hamiltonian (36), and in the next stage of the calculations one uses for the mixing of the states the Hamiltonian

$$H_{\text{mix}} = \alpha\,(s_\pi^+ s_\pi^+ + s_\pi s_\pi) + \beta\,(d_\pi^+ d_\pi^+ + d_\pi d_\pi)^{(0)} \qquad (59)$$

and diagonalizes $H + H_{\text{mix}}$ in the basis of the lowest configurations n_π and $n_\pi + 2$. At this stage, the energies of the states of the $n_\pi + 2$ configurations are augmented by the energy ΔE, which corresponds to the excitation energy of this configuration.[1)]

In the calculation, the values of the parameters of the Hamiltonian, χ_ν and $c_{\nu L}$, which depend only on n_ν, are taken to be the same for the two configurations. For the $E2$-transition operator the following expression is used:

$$\hat{T}(E2) = e^*(1)\,(Q_{1\pi} + Q_{1\nu}) + e^*(3)\,(Q_{3\pi} + Q_{3\nu}), \qquad (60)$$

where $e^*(1)$ and $e^*(3)$ are the effective charges for the first and second configurations, and the operators Q_π and Q_ν are expressed in terms of the boson operators as in (41). The expression given above for $\hat{T}(E2)$ is written down under the assumption of equality of the effective charges for the proton and neutron bosons.

As an example, we consider the main results of the use of this approach for the calculation of the structure of the low states of ^{112}Cd and ^{114}Cd. Figure 25 shows the results of calculations of the energies of the excited states of ^{112}Cd and the $B(E2)$ values for transitions between them in accordance with the data of Ref. 74. It follows from the experimental data that in the region of the triplet states two additional levels, 0^+ and 2^+, are observed, whose positions cannot be explained in the framework of the ordinary IBM. At the same time, the model that takes into account the presence of the two configurations correctly reproduces, as follows from the figure, not only the positions of these levels but also the $E2$-transition probabilities for the complete set of states in the considered region of energies and also the quadrupole moment of the 2_1^+ state. Analogous results were obtained in the same study for ^{114}Cd. The appearance of such "extra-states" in the region of the triplet energies of precisely the isotopes ^{112}Cd and ^{114}Cd is not fortuitous. It follows from the calculations that the excitation energy (ΔE) of the configurations with $n_\pi = 3$ relative to the $n_\pi = 1$ configuration is 5.5 MeV; at the same time, it can be seen from the figure that the energy of the ground state of the configuration with $n_\pi = 3$ does not exceed 1.5 MeV. This is due to the fact that the binding energy of the configuration with $n_\pi = 3$ is appreciably greater than the binding energy of the configuration with $n_\pi = 1$. The binding energy is determined by the quadrupole-quadrupole interaction of the protons and neutrons, so that for $n_\pi = 3$ it is greater than for $n_\pi = 1$. It becomes maximal in the middle of the shell, where the number of bosons is maximal. With increasing distance from the middle of the shell, the excitation energy of the "extra-states" increases and enters the region of the triplet states. It is an interesting circumstance that in the case of Cd the presence of the 0^+ and 2^+ extra-states associated with the $n_\pi = 3$ configuration did not lead to a significant change in the properties of the ground, 2_1^+, and 4_1^+ states [in the values of the energies, $B(E2)$, and $Q(2_1^+)$].

An analogous approach was used in Ref. 75 to calculate the structure of the excited states of the molybdenum isotopes. If one considers the $Z = 40$ subshell, the normal configuration in the framework of the IBM is characterized for the Mo isotopes by the number $n_\pi = 1$ of the proton bosons. If, however, one takes into account the possible excitation of a pair of protons through a subshell and the corresponding formation of two proton holes within it, then $n_\pi = 3$ in such a case.

Calculations of the structures of the low-lying states of the isotopes $^{96\text{-}104}$Mo were made in the study on the basis of the formalism presented above. The values of ΔE adopted in the calculations decrease with increasing number of neutrons, and the values of the parameters α and β were taken

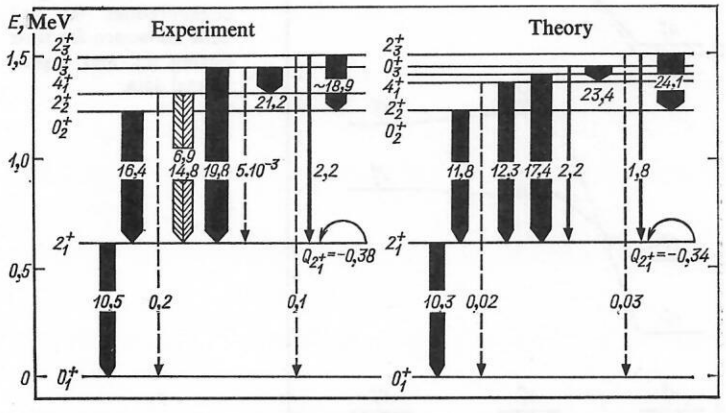

FIG. 25. Comparisons of calculations of the structure of the nucleus ^{112}Cd in the IBM-II, with allowance for configuration mixing in accordance with the data of Ref. 74, with experimental data. The values of $B(E2)$ are measured in units of $10^{-2}e^{-2}\cdot b^2$, and $Q(2_1^+)$ in units of $e\cdot b$.

[1)]The idea of nonconservation of the boson number was also advanced by E. Nadzhakov (Nadjakov).[73]

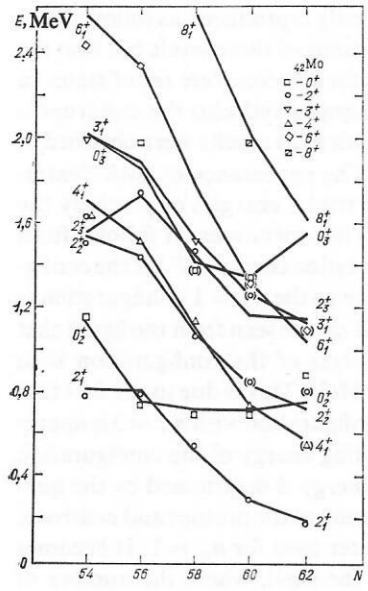

FIG. 26. Comparison of calculated energies of excited states of Mo isotopes, obtained in the IBM-II with allowance for configuration mixing,[75] with experimental data.

equal to 0.16. In Fig. 26, the calculated values of the excited states of the Mo isotopes with $E < 2.5$ MeV are compared with the experimental data. It follows from the data of the calculations that the influence of the configuration mixing (the importance of the term H_{mix}) is small in the case of the isotopes ^{96}Mo, ^{102}Mo, and ^{104}Mo but is very large for ^{98}Mo and ^{100}Mo. The effect of the mixing for these isotopes is illustrated in Fig. 27. In the figure, the state spectra calculated for each of the configurations without allowance for their mixing (i.e., setting $\alpha = \beta = 0$) are represented by the lines of column I. The numbers 1 and 3 indicate that the states belong to the configuration with $n_\pi = 1$ or with $n_\pi = 3$ proton bosons. In column II we give the calculated energies obtained with allowance for the configuration mixing. In column III we give the experimental energies. It follows from Fig. 27 that the usual calculations made in the framework of one normal configuration with $n_\pi = 1$ lead to very large distances between the levels, in disagreement with the experimental data. Thus, the calculated energy of the 2_1 state of ^{98}Mo is 1.4 MeV. At the same time, the calculations that take into account the existence of two configurations and their mixing correctly describe the spectrum of the low-lying states and, in particular, the anomalously low position of the 0_2^+ states. It can also be seen from Fig. 27 that, in contrast to the situation in the ^{112,114}Cd isotopes, allowance for the configuration mixing strongly influences the position and mutual disposition of the levels. In this case, the results of the calculation of the probabilities of the electromagnetic transitions and their comparison with experiment are particularly important for the comprehensive testing of the viability of the proposal of configuration mixing. In Ref. 75, the values

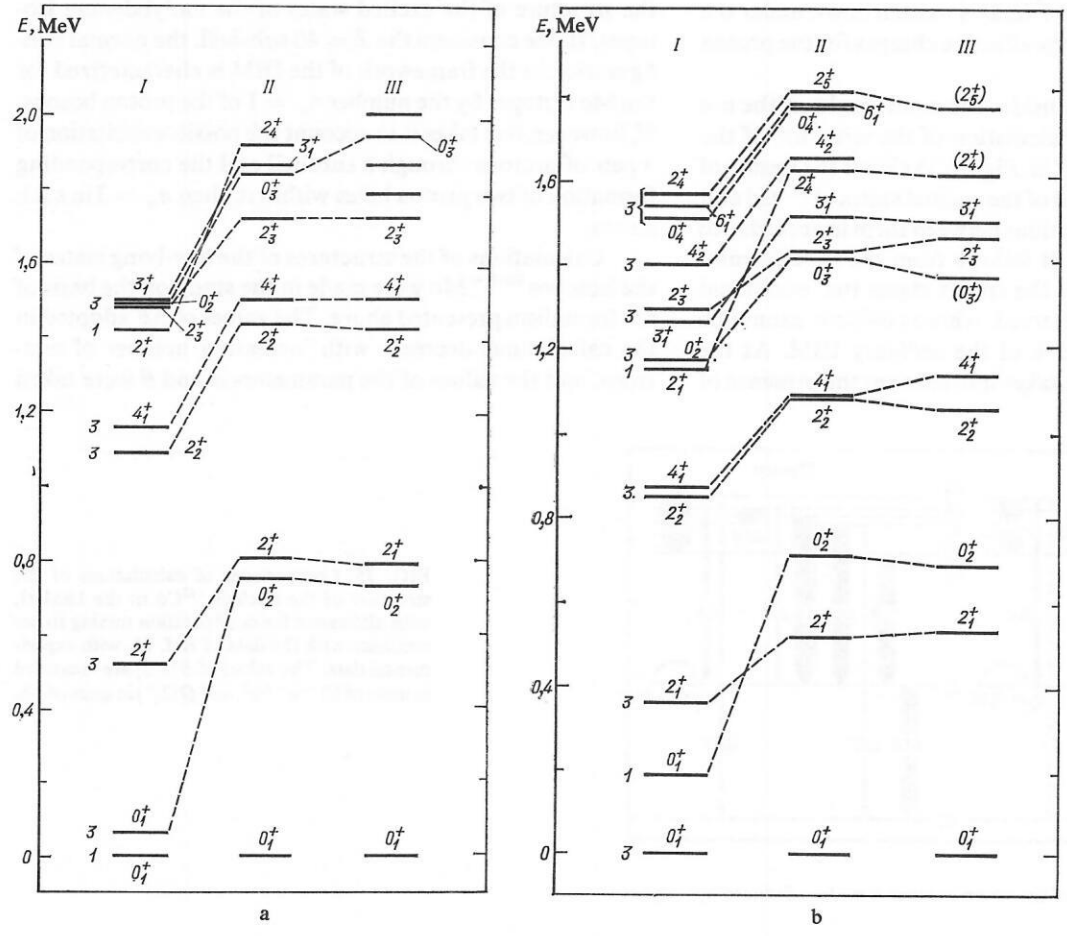

FIG. 27. Calculated energies of excited states of ^{98}Mo and ^{100}Mo without allowance for mixing of configurations (a) and with allowance for their mixing (b), and experimental data.

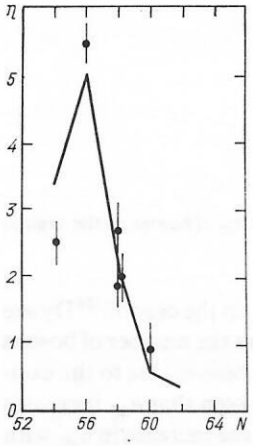

FIG. 28. The ratio $\eta B(E2; 0_2^+ \to 2_1^+)/B(E2; 2_1^+ \to 0_1^+)$ for Mo isotopes.

of a number of $B(E2)$ ratios were calculated. It was assumed that the ratio $e^*(3)/e^*(1)$ [see (60)] of the effective charges is 2. In addition, setting $e^*(1) = 0.053e\cdot b$, Sambataro and Molnár[75] also calculated the values of $B(E2; 0_2^+ \to 2_1^+)$ and $Q(2_1^+)$. The agreement with experiment was entirely satisfactory. Figure 28 shows the ratios $\eta = B(E2; 0_2^+ \to 2_1^+)/B(E2; 2_1^+ \to 0_1^+)$ for various Mo isotopes. It can be seen that the calculated value of η for ^{100}Mo ($N = 58$) is close to the experimental value ($\eta > 5$).

Having noted the successful description of the properties of the Mo isotopes on the basis of the IBM-II modification that takes into account the mixture of the one- and three-proton boson configurations, we point out that a successful description of the properties of these same isotopes was given almost ten years ago by Jolos *et al.* in Ref. 54, in which it was shown that the IBM-I can explain the lowering of the 0_2^+ states. Of course, in the framework of the usual variant of the IBM-I it is impossible to explain the existence of two 2^+ levels with very nearly the same energy, for example, 1.93 and 2.09 MeV, as is observed in ^{96}Mo. However, when allowance is made for the coupling of the quadrupole and pairing vibrations, as was done in Ref. 55, the energies of the levels and the transition probabilities in ^{96}Mo can be calculated in satisfactory agreement with experiment, as is indicated by the data in Table IX. Thus, in the framework of the IBM-I there are also ways of describing situations that go beyond the possibilities of its usual formulation.

A method of mixing configurations with one and three proton bosons was used in Ref. 76 to calculate the properties of Zn isotopes. However, as follows from Fig. 20, which gives the results of calculations in the framework of the IBM-I, and the data of Ref. 76, this approach does not lead in the given case to results better than when the ordinary variant of the IBM-I is used.

One of the main differences of the IBM from the other collective models is its assumption of a finite number of bosons, and, as a consequence of this, it is not possible to have excitation of states with $I > 2n$ and a decrease in the $B(E2; I \to I+2)$ values beginning at some value of I.

So far, there have been no clear experimental proofs of the existence of the above cutoff effect with respect to the boson number. In this connection, it is desirable to consider the possibility of including in the IBM additional degrees of freedom to eliminate or weaken this effect.

One such possibility is to take into account pairs of nucleons coupled into bosons with angular momentum $L > 2$, above all, g bosons. Their importance increases with increasing I, and their introduction affects the increase in the $B(E2)$ values for transitions between high-spin states.

Another possibility is through the approach of Duval and Barrett discussed above.[72] In Ref. 77, this approach was used to interpret the results of an investigation of the high-spin states of the even isotopes of Dy [energies and $B(E2)$ values], published in Ref. 78. In contrast to Ref. 72, the study of Ref. 77 took into account not only $2p$–$2h$ excitations, which lead to two additional bosons, but also $4p$–$4h$ and $6p$–$6h$ excitations, which are equivalent to four and six additional bosons. The calculations were made in the framework of the IBM-I, and the Hamiltonian used contained only four parameters ($\varepsilon, \varkappa, \varkappa', \varkappa''$):

$$H = \varepsilon \hat{n}_d - \varkappa \tilde{Q}\tilde{Q} + \varkappa' \hat{I}^2 + \varkappa'' P^+ P, \tag{61}$$

where $\tilde{Q}$ is the quadrupole operator of the SU(3) algebra (28), and P^+ is a pairing operator invariant under $O(6)$ transformations, so that the term P^+P of the Hamiltonian can be expressed in terms of the Casimir operator of the $O(6)$ algebra:

$$P^+ = \sum_\mu d_\mu^+ d_{\bar{\mu}}^+ - s^+ s^+. \tag{61a}$$

With allowance for the nonconservation of the boson number, the basis functions were chosen in Ref. 77 in the form

TABLE IX. Calculated and experimental energies of ^{96}Mo states, in MeV, and relative $B(E2)$ values in accordance with the data of Refs. 54 and 55.

I	Energy		I_i	I_f	$B(E2; I_i \to I_f)/B(E2; 2_1^+ \to 0_1^+)$	
	Experiment	Theory			Experiment	Theory
4_1^+	2,09	2,08	0_2^+	2_1^+	2,4±0,3	2,4
2_3^+	2,09	2,10	4_1^+	2_1^+	1,8±0,4	1,9
2_2^+	1,93	2,02	2_2^+	2_1^+	0,8±0,2	0,94
0_2^+	1,48	1,28	2_3^+	2_1^+	0,8±0,2	0,74
2_1^+	1,00	1,00	2_2^+	0_2^+	0,06	0,11
0_1^+	0,00	0,00	2_2^+	0_2^+	—	0,53

$$|(sd)^n\rangle \oplus |(sd)^{n+2}\rangle \oplus |(sd)^{n+4}\rangle \oplus (sd)^{n+6}\rangle, \quad (62)$$

where $|(sd)^n\rangle$ denotes the eigenfunctions for the configuration with total number of s and d bosons equal to n.

For the mixing of states differing by two bosons, the authors used the Hamiltonian H_{mix} (59), as in Ref. 72, making no distinction between proton and neutron bosons. The values of the parameters $\varkappa$, $\varkappa'$, and $\varkappa''$ were optimized by means of the energies of the excited states of the Dy isotopes. The parameters α and β in H_{mix} and the parameter χ_{E2} of the $E2$-transition operator were fitted using the $B(E2)$ values for transitions in the yrast band. In the calculations, it was assumed that the energy shift ΔE of the configuration with the two additional bosons is 2.1 MeV, and for configurations with four and six bosons 2 and 3 times greater.

With increasing number of particle-hole excitations and, accordingly, number of additional bosons, the excitation bands of the states of the corresponding configurations acquire an ever stronger rotational nature. The transition of the expression (61) to the SU(3) limit is achieved by decreasing the contribution of the perturbing term $\varepsilon\hat{n}_d$. To this end, it is assumed in the calculations that $\varepsilon = (n_{\max} - n_i)\theta$, where $n_{\max} = n + 6$, $n_i = n + 2i$, $i = 0, 1, 2, 3$, and n is the initial number of bosons in the absence of excitation of the basic particles. The value of θ is taken to be 0.0625 MeV.

Figure 29 gives the results of the calculation of the dependence of $I_x = I + 1/2$ on the rotation frequency for ^{158}Dy in a comparison with experimental data. It can be seen that allowance for excitation of the core nucleons makes it possible to describe in the framework of the IBM the structure of the high-spin states of the ground-state band and its interaction with the bands of a more complicated nature in the region of the backbending (near $I = 16$).

The calculations also make it possible to find the effective number of bosons, which is determined by the expression

$$n_{\text{eff}}(I) = \sum_{n'=n}^{n+6} n'\phi(I, n'), \quad (63)$$

where $\phi(I, n')$ is the amplitude of the component with number of bosons n' of the wave function of the state with spin I.

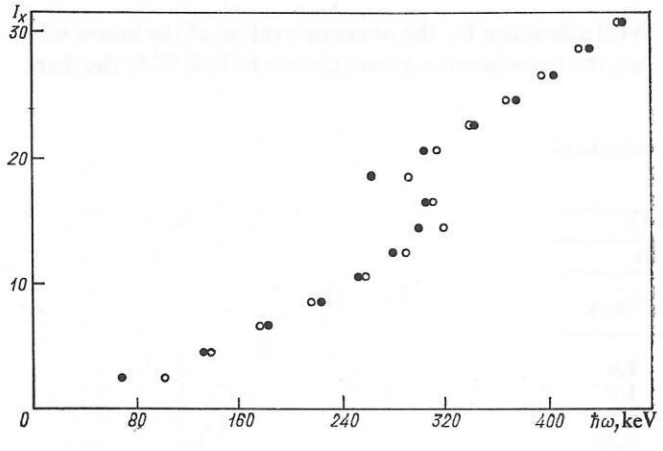

FIG. 29. Dependence of the moment I_x on the rotation frequency ω for ^{158}Dy. The open circles represent the calculation, and the black circles are the experimental data.

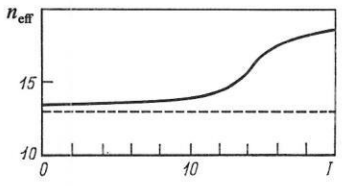

FIG. 30. Dependence of the effective number n_{eff} of bosons on the angular momentum I.

The results of calculations of n_{eff} in the case of ^{158}Dy are given in Fig. 30. The broken line shows the number of bosons without allowance for the additional bosons due to the excitation of the core particles. It can be seen that n_{eff} increases sharply with increasing I. Of course, the increase in n_{eff} with I greatly weakens the effect of the cutoff with respect to the number of bosons.

In Fig. 31, calculated values of $B(E2)$ for transitions between yrast states are compared with experimental data, indicated by the crosses. The calculation reproduces well the general behavior of the $B(E2)$ values for states with I up to 30 and the influence of the backbending on the $B(E2)$ values at $I = 16$, though the schematic nature of the model does not, of course, permit reproduction of the finer details of the results.

Thus, it follows from consideration of the results of Ref. 77 that allowance for the excitation of intracore particles on the basis of mixing of configurations with different numbers of bosons makes it possible to describe in a unified manner in the framework of the IBM the behavior of the energies of high-spin states (including the backbending effect) and the values of the reduced probabilities of $E2$ transitions, and to demonstrate the possible weakening of the effect of the cutoff with respect to the number of bosons as a result of an increase in the effective number of bosons.

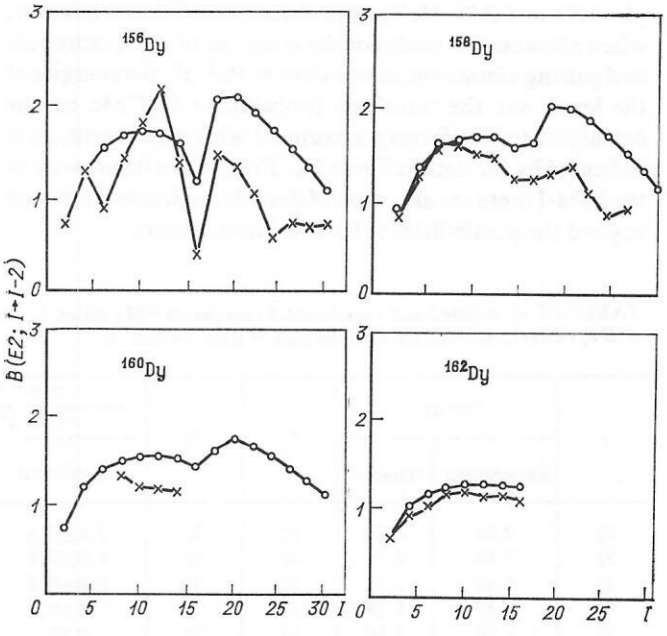

FIG. 31. Values of $B(E2; I \to I-2)$ for transitions in yrast bands of the isotopes $^{156-162}$Dy. The experimental data are indicated by crosses.

10. ALLOWANCE FOR DIFFERENT TYPES OF PROTON BOSONS

An example of a modification of the IBM-II is also Ref. 64, mentioned above, in which the properties of low excited states of the Ge isotopes were calculated. The modification of the IBM-II in Ref. 64 consists of the assumption that the structure of these states is determined by the presence of two proton configurations (with the same number of bosons). The configuration with the lowest energy corresponds to four valence protons (above the $Z = 28$ shell) being basically in the $p_{3/2}$ state. (The corresponding bosons are denoted by s_π, d_π.) However, because of the effects of neutron-proton pairing, which increases with the number of neutrons, there is a tendency for pairs of protons to be transferred to levels with large values of the angular momentum ($f_{5/2}$, $g_{9/2}$) and to the development of deformation.[79] The bosons corresponding to these pairs (for which the notation s'_π, d'_π is introduced) form the second configuration.

The parameters of the Hamiltonian that relate to the first configuration (s_π, d_π) were determined by comparing the calculated and experimental energies of the lowest $^{68}_{32}Ge_{36}$ levels; the parameters of the second configuration (s'_π,d'_π) were determined by fitting to the energies of the lowest $^{76}_{32}Ge_{44}$ states. An operator of the interaction of these two configurations was then introduced,

$$H_{\text{mix}} = \alpha\,(s^+_\pi s'_\pi + s'^+_\pi s_\pi) + \beta\,[(d^+_\pi d')^{(0)} + (d'^+_\pi d_\pi)^{(0)}], \quad (64)$$

and also an additional parameter δE, which determined the energy difference between the unperturbed states of the two configurations. In Ref. 64, it was assumed that δE varies linearly with the number of neutrons. In the calculations of $B(E2)$, it was assumed that each configuration is characterized by its own effective charge, $e^*(1)$ and $e^*(2)$, with $e^*(2)/e^*(1) = 2$. The value of $e^*(1)$ was chosen to make the calculated $B(E2; 2_1^+ \to 0_1^+)$ value agree with the experimental value in ^{72}Ge.

In Fig. 32, the calculated energies of the excited states of Ge isotopes with $A = 66$–78 are compared with experimental data. As a rule, the results of the calculations of different studies agree well with one another. Some differences are specially noted in Fig. 32. It is interesting to note that, despite the difference between the theoretical approaches, in several of the studies the existence of two 2^+ states in the region 1.5–1.8 MeV is predicted. At the present time, only one state is known experimentally in this region. The calculated values of $B(E2)$ and $Q(2_1^+)$ are given in Table III, where they are compared with the experimental values. It can be seen that the calculated $B(E2)$ values agree with one another and with the experimental data. An achievement of Ref. 64 was the correct description of the $Q(2_1^+)$ values for all Ge isotopes, though the description of the $B(E2)$ values for transitions to or from the 0_2^+ level in Ref. 64 is not as good as the description achieved in the IBM-I and in Ref. 53. Another success of Ref. 64 is the qualitatively correct description of the behavior of R, the ratio of the cross sections of the (p, t) and (t, p) reactions with excitation of 0_1^+ and 0_2^+ states (Fig. 33).

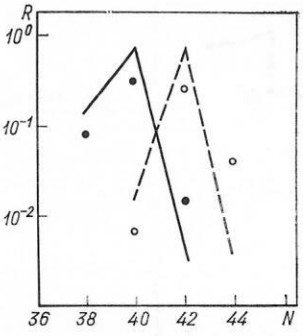

FIG. 33. Ratios of cross sections of the reactions (p, t) (black circles for the experiment, continuous line for the theory) and (t, p) (open circles for the experiment, broken line for the theory) with excitation of 0_1^+ and 0_2^+ states of Ge isotopes in accordance with the data of Ref. 64.

The examples given above show that in some cases the introduction of two configurations and their interaction makes it possible to describe in a nucleus the coexistence of different collective structures, these being manifested, in particular, in the form of extra-states. It should, however, be

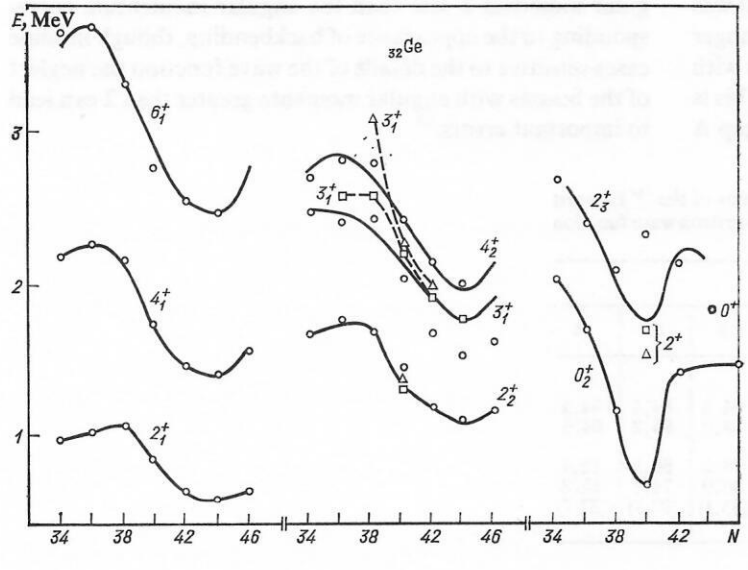

FIG. 32. Comparison of the calculated energies of excited states of the isotopes $^{66-78}$Ge, as found in various studies, with experimental data. The open circles are the experimental points, the continuous curves are the IBM-I calculation, the open triangles are the data of Ref. 53, and the open squares are the data of Ref. 64.

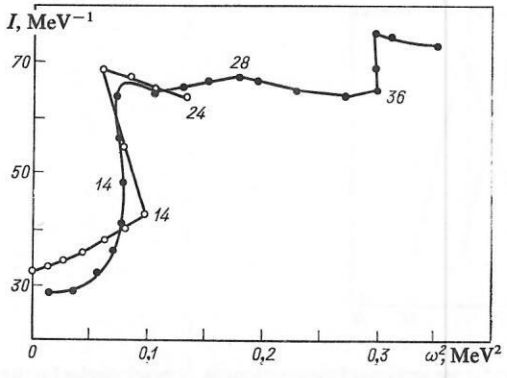

FIG. 34. Dependence of the moment of inertia I on the square of the rotation frequency for ^{164}Er.

noted that the use of this approach is associated with the introduction of a large number of additional parameters. Besides the parameters of the basic IBM-II Hamiltonian, the parameters listed above, α, β, and δE, are also used in the calculations for the second configuration. Therefore, in actual calculations one attempts to reduce the number of parameters to a minimum by making a number of simplifying assumptions, whose validity must be tested as well. It must also be clarified to what extent the mechanism proposed for the occurrence of another configuration applies in the case of other shells and subshells. Also unclear is the degree of justification and the region of applicability of the new configuration as the result of the transition of two protons from one above-shell orbital to another, as proposed in Ref. 72.

11. DESCRIPTION OF DEFORMED NUCLEI IN THE FRAMEWORK OF THE IBM

We now consider the possibility of using the IBM to describe deformed nuclei. The model encounters difficulties in the description of high-spin states, this being due to the fact that only s and d bosons are taken into account. In terms of the microscopic basis of the model, this means that one takes into account only those fermion pairs that have angular momentum $L = 0$ and 2 (S and D pairs). The errors in the description of the fermion system by means of only S and D pairs have been considered in a number of studies.[80–82] It was shown that the restriction to S and D pairs leads to a stronger spreading of the Fermi level than in the case when pairs with all possible angular momenta are taken into account. This is the cause of other errors—the overestimation of the gap Δ and the decrease in the intrinsic quadrupole moment. Since the value of Δ has a strong influence on the moment of inertia, doubt arises as to whether it is possible in the framework of the IBM (i.e., boson mapping of S and D pairs) to describe successfully the rotational spectra of deformed nuclei. However, the calculations made in Ref. 83 for ^{164}Er give grounds for a certain optimism.

The model used in Ref. 83 has a realistic behavior of the single-particle levels, and it contains quadrupole particle-hole forces and a monopole pairing. Calculations were made on the basis of the cranking model with Hartree–Fock–Bogolyubov (HFB) self-consistency. The calculated values of the moment of inertia are given as functions of ω^2 in Fig. 34, from which it follows that entirely satisfactory agreement with experiment is achieved. The proton and neutron HFB functions were then projected onto functions $|\Phi_{2n}(I)\rangle$ with a definite particle number:

$$|\Phi_{2n}(I)\rangle = \left(\sum B_{KK'} a_K^+ a_{K'}^+\right)^n |0\rangle, \tag{65}$$

where n is the number of pairs of valence nucleons. After this, each operator of the pair $(\Sigma B_{KK'} a_K^+ a_{K'}^+)$ was expanded with respect to states with a definite angular momentum:

$$\sum B_{KK'} a_K^+ a_{K'}^+ = \sum_{L=0,2,4\ldots} A_L (a^+ a^+)^{(L)}. \tag{66}$$

The calculations show that the proton-pair function preserves SD dominance in a very wide range of spins, though the alignment of two neutrons in an $i_{13/2}$ state has the consequence that at spins $I > 12$ the contribution of the SD pairs to the total neutron function decreases, and at $I = 16$ a two-quasiparticle pair with angular momenta L equal to 10 and 12 is distinguished. Table X gives the total contributions from the S, D, and G pairs to the total wave function. It can be seen from the table that the structure of the proton states is exhausted in a wide interval of angular momenta by S, D, and G pairs, the contribution of the G pairs being of order 10%. The G pairs make a somewhat larger contribution (about 20%) to the structure of the neutron state. Thus, allowance for only S and D pairs in the fermion space (and the corresponding bosons in the IBM) can give in the general features a correct picture of the properties of states with angular momenta I less than the angular momentum corresponding to the appearance of backbending, though in some cases sensitive to the details of the wave function the neglect of the bosons with angular momenta greater than 2 can lead to important errors.[84]

TABLE X. Total contribution of SDG states (%) to wave functions of the ^{164}Er yrast states. (In brackets the contribution of the SDG + OM states to the neutron wave function is shown.) The data are taken from Ref. 83.

Configuration	I								
	0	2	4	6	8	10	12	14	16
Protons									
$S+D$	88,1	87,4	87,4	86,8	85,6	85,0	84,4	84,4	84,4
$S+D+G$	99,3	98,6	98,6	97,9	97,2	96,6	95,9	95,2	94,5
Neutrons									
$S+D$	77,2	77,2	75,7	74,1	72,6	70,7	68,3	56,5	12,4
$S+D+G$	98,1	98,1	96,8	95,5	94,3	92,4	90,0 (93,1)	74,1 (93,7)	15,8 (87,7)

In conclusion, we consider in somewhat more detail studies in which the applicability of the IBM for describing the properties of deformed nuclei has been studied by comparing the results of calculations in the framework of the IBM with experimental data. For the majority of deformed nuclei, the number of bosons is fairly large. For example, for $^{168}_{68}$Er the numbers of proton and neutron bosons are 7 and 9, respectively. Under such conditions, the procedure of the calculations in the framework of the IBM-II is complicated appreciably, and in practice the analysis has been done using the IBM-I in a simplified variant in which the less important terms in the IBM-I Hamiltonian are ignored.

In 1981, a collaboration between physicists from Canada, France, Great Britain, and the United States resulted in the publication of Ref. 85, which contains a detailed study of the decay scheme of ^{168} Er obtained in the reaction ^{167}Er(n, γ) ^{168}Er. The use of diverse techniques with unique capabilities in the investigations, in particular a crystal-diffraction spectrometer having a high resolution and the capability of detecting very weak transitions, and also the technique of averaging resonance cross sections, made it possible to detect in the region of excitation up to 2 MeV all states with spin $I \leqslant 6$ and to observe many low-intensity transitions. In the subsequent papers of Refs. 86 and 87, the material of these studies was used for detailed comparison of the capabilities of the geometrical model and the IBM when applied to deformed nuclei.

We note that until recently the judgement about the capabilities of the IBM has been based on the successes in the global description of the overall properties of isotopes or families of them, and particular attention has not, as a rule, been paid to the deviations from the predictions of the model that do exist, this possibly being due to the absence of other approaches with comparable success in describing the structure of the nuclei considered, and also to the absence of nuclides with a structure comprehensively studied.

As was shown in Sec. 2, in the SU(3) limit the bands within one (λ, λ) multiplet are degenerate [i.e., $E(2_\beta^+) = E(2_\gamma^+)$], and if as the $E2$-transition operator one takes e^*Q (28), then transitions between states with different values of (λ, λ) are forbidden, in particular, transitions from the β and γ bands to the ground-state band. Neither of these conclusions corresponds to the real situation. To lift the degeneracy in the Hamiltonian (27), one frequently adds the term $\varkappa'' P^+ P$, and the parameter $\varkappa''$ is chosen to achieve the best agreement for the existing set of states:

$$H = -\kappa \tilde{Q}\tilde{Q} + \kappa' \hat{I}^2 + \kappa'' P^+ P. \tag{67}$$

In Ref. 90, the $E2$-transition operator was represented by the expression

$$\hat{T}_\mu(E_2) = e^* Q_\mu = e^* \left[d_\mu^+ s + s^+ d_{\tilde{\mu}} + \frac{R}{\sqrt{5}} (d^+ d)_\mu^{(2)} \right]. \tag{68}$$

The factor $R/\sqrt{5}$ in (68) replaces the parameter χ_{E2} in (22).

To reproduce the necessary strength of the transitions, the parameter R was varied to make the calculated value of $B(E2; 2_2^+ \to 0_1^+)/B(E2; 2_1^+ \to 0_1^+)$ agree with the experimental value. Thus, in this approach there are five parameters, one of which $(\varkappa'')$ is fitted to the set of data, while the remainder are calculated on the basis of the experimental $E(2_1^+)$, $E(2_2^+)$, $B(E2; 2_1^+ \to 0_1^+)$, and $B(E2; 2_2^+ \to 0_1^+)$ values.

In Fig. 35, the levels of ^{168}Er with positive parity are compared with their calculated values. It can be seen that the calculations reproduce all the bands observed experimentally and situated below the gap, together with their order and all states within the bands. An exception is the $K^\pi = 3^+$ band at 1635 keV. To explain its position, one must include g bosons.

In a detailed examination of the situation, it is found, however, that there are a number of discrepancies with experiment. The bases of the $2_1^+, 0_2^+, 0_3^+, 2_2^+$ bands differ by

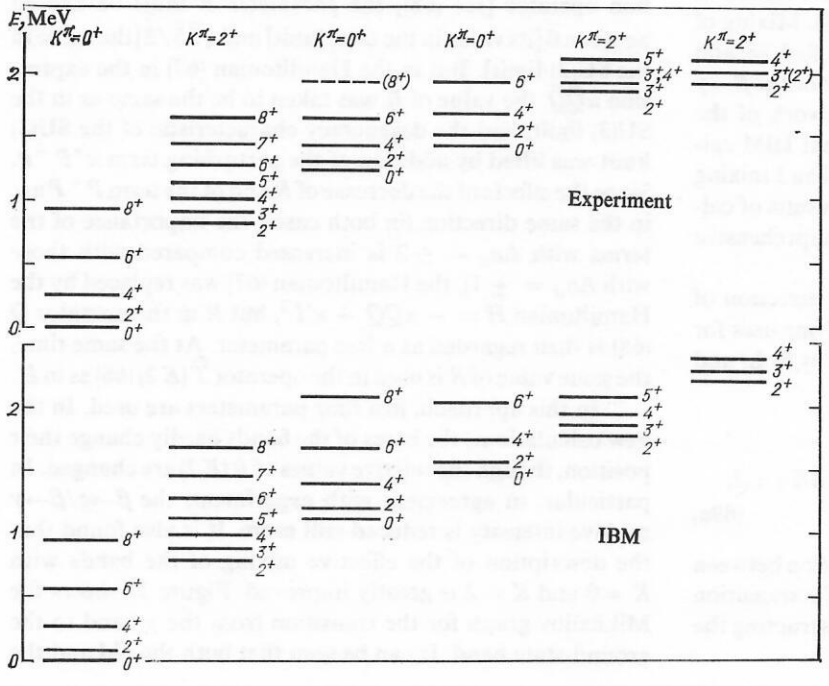

FIG. 35. Calculated and experimental energies of ^{168} Er levels.

21, 93, 58, 83 keV, respectively, the 2_3^+ band with base energy 1930 keV corresponds in the calculation to 2200 keV, and, finally, the base of the band with $K^\pi = 4^+$ and with $E = 1610$ keV corresponds to a calculated energy 2030 keV. It should also be noted that the IBM does not reproduce the increases by about 25% in the moment of inertia in the β band, although this can be achieved by adding terms to the Hamiltonian.

All these discrepancies are absent in the geometrical model, since the use of the formula of the rotational model, $E_I = E_0 + AI(I+1) + BI^2(I+1)^2$, which, it is true, does require three parameters for each band in order to describe the energies, leads to excellent agreement with experiment (the discrepancy is only 5–20 eV).

Of particular interest is a comparative study of the $E2$-transition probabilities. In Ref. 86, the calculated $B(E2)$ values are compared with the experimental data for transitions from states of the γ, β, and 0_3^+ bands. The results of the calculations for the γ and β bands agree well with the experimental data. In the case of the 0_3^+ band, the discrepancies are much larger, but they almost all occur when the calculated absolute values of $B(E2)$ are 0.01 or several thousandths of the single-particle estimate. It is obvious that comparatively small perturbations of these purely collective effects can explain the observed discrepancies. It follows from the results of the calculations that the $\beta \to \gamma$ transitions predominate over the transitions from the β band to the ground-state band. This is a natural conclusion from the point of view of the IBM. In the SU(3) limit, the transition $\beta \to g$ is forbidden altogether, while the $\beta \to \gamma$ transition is not, since it is a transition that does not change (λ, λ). This rule is weakened with decreasing R [see (68)]. Conversely, in the purely geometrical model the $\beta \to \gamma$ transitions are forbidden.

It is well known that the Alaga rules are not strictly satisfied in the geometrical model, and a significant improvement in the description of the actual values of the branching ratios can be achieved by taking into account mixing of the γ and g bands and of the β and g bands. Mixing of the β and γ bands was also taken into account in Ref. 86, and it was shown that in this case the predominance of the $\beta \to \gamma$ transitions can also be described in the framework of the geometrical model. The comparison showed that IBM calculations not related to additional ideas about band mixing agree with the experiments no worse than the results of calculations in the geometrical model with comprehensive allowance for the mixing coefficients.

However, one can go even further in the direction of detailed analysis of the reduced probabilities if one uses for their analysis the Mikhaĭlov graph, as proposed by Bohr and Mottelson (see Ref. 87). Noting that

$$B(E2;\ I_1K_1 \to I_2K_2) = 2\,(C^{I_2K_2}_{I_1K_12\Delta K})^2 \times \{M_1 + M_2[I_2(I_2+1) - I_1(I_1+1)]\}^2, \quad |\Delta K| = 2, \tag{69a}$$

where M_1 is the matrix element of the $E2$ transition between bands, and M_2 is the matrix element of the $E2$ transition associated with the admixture of states, and constructing the dependence

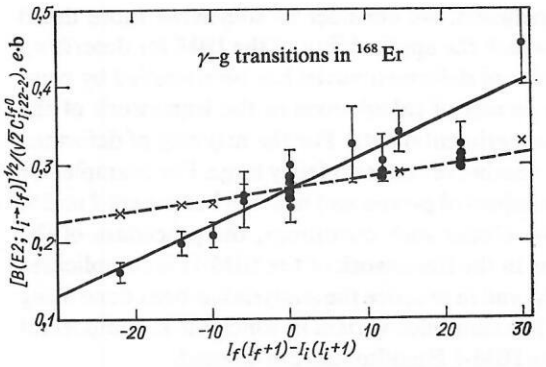

FIG. 36. The Mikhaĭlov graph (69b) calculated using a Hamiltonian in the form (67). The crosses are the IBM results, and the black circles and triangles are the experimental data.

$$[B(E2;\ I_1K_1 \to I_2K_2)]^{1/2}\,\frac{1}{\sqrt{2}}\,(C^{I_2K_2}_{I_1K_1,\,2\Delta K})^{-1} = f(x), \qquad x = I_2(I_2+1) - I_1(I_1+1), \tag{69b}$$

we see that the slope of the line gives M_2 and the intercept with $x = 0$ gives the value of M_1.

The results of such an analysis for the experimental and calculated values of $B(E2)$ in the case of $\Delta K = 2$ transitions are shown in Fig. 36. The calculated values were found using the IBM. The experimental $B(E2)$ values were determined from the relative values and the assumption that the quadrupole moment of the β and γ bands does not differ from Q_0 for the ground-state band of ^{168}Er and is $7.6 \times 10^2 e \cdot \mathrm{F}^2$ [for the 2_γ^+ state, the absolute intensities are based on measurements of $B(E2; 0_g^+ \to 2_\gamma^+)$ in Coulomb-excitation studies]. As can be seen from Fig. 36, the Mikhaĭlov graphs using the experimental data and the values calculated in the IBM differ appreciably.

The improvement of the IBM formalism used in Ref. 88 made it possible, however, to improve the agreement with experiment. It has already been noted that in the $E2$-transition operator [see (68)] the parameter R must be chosen between 0 [its value in the $O(6)$ limit] and $\sqrt{35}/2$ [the value in the SU(3) limit]. But in the Hamiltonian (67) in the expression $\varkappa \tilde{Q}\tilde{Q}$ the value of R was taken to be the same as in the SU(3) limit, and the degeneracy characteristic of the SU(3) limit was lifted by addition of the perturbing term $\varkappa'' P^+ P$. Since the effects of the decrease of R and of the term P^+P are in the same direction (in both cases, the importance of the terms with $\Delta n_d = \pm 2$ is increased compared with those with $\Delta n_d = \pm 1$), the Hamiltonian (67) was replaced by the Hamiltonian $H = -\varkappa QQ + \varkappa' I^2$, but R in the operator Q (68) is then regarded as a free parameter. At the same time, the same value of R is used in the operator $\hat{T}(E2)$ (68) as in H.

In this approach, just four parameters are used. In the new calculations, the bases of the bands hardly change their position, though the relative values of $B(E2)$ are changed. In particular, in agreement with experiment, the $\beta \to g / \beta \to \gamma$ relative intensity is reduced still more. It is also found that the description of the effective mixing of the bands with $K = 0$ and $K = 2$ is greatly improved. Figure 37 shows the Mikhaĭlov graph for the transition from the γ band to the ground-state band. It can be seen that both the old and the

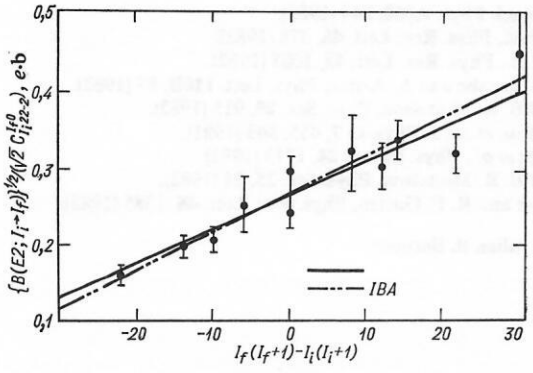

FIG. 37. Mikhaĭlov graph plotted using the data of Ref. 88. The chain line is in accordance with the IBM, and the black circles are the experimental data.

new calculations in the framework of the IBM-I are well represented by straight lines, but in the new formalism the straight line through the calculated data hardly differs from the one through the experimental points, so that the effective value of the matrix element associated with the band mixing is well reproduced by the theory.

Investigation of the applicability of the IBM-I for the description of the properties of ^{168}Er was an important step in the experimental verification of the theory. It had long been shown that the IBM describes satisfactorily the general features in the behavior of many nuclei. However, the results of the investigation of ^{168}Er made possible a detailed verification of the applicability of the IBM, in the course of which it was demonstrated that a small number of terms taking into account the boson interaction permits description of a large number of data.

[1]R. V. Jolos and D. Janssen, Fiz. Elem. Chastits At. Yadra **8**, 330 (1977) [Sov. J. Part. Nucl. **8**, 138 (1977)].
[2]R. V. Jolos and D. Janssen, Preprint R4-9339 [in Russian], JINR, Dubna (1975).
[3]R. V. Jolos and V. Rybarska, Fiz. Elem. Chastits At. Yadra **3**, 739 (1972) [Sov. J. Part. Nucl. **3**, 377 (1972)].
[4]R. V. Jolos, F. Dönau, and D. Janssen, Teor. Mat. Fiz. **20**, 112 (1974).
[5]F. Dönau, D. Janssen, and R. V. Jolos, Nucl. Phys. **A224**, 93 (1974).
[6]R. V. Jolos, F. Dönau, and D. Janssen, Yad. Fiz. **22**, 965 (1975) [Sov. J. Nucl. Phys. **22**, 503 (1975)].
[7]D. Janssen and R. V. Jolos, Soobshchenie (Communication) E4-8992, JINR, Dubna (1975); R. V. Jolos and D. Janssen, Izv. Akad. Nauk SSSR, Ser. Fiz. **40**, 1273 (1976); G. Holzwarth *et al.*, Nucl. Phys. **A261**, 1 (1976).
[8]T. Holstein and H. Primakoff, Phys. Rev. **58**, 1098 (1940).
[9]J. Schwinger, The Quantum Theory of Angular Momentum (eds. L. C. Biedenharn and H. van Dam), Academic Press, New York (1962).
[10]V. M. Mikhaĭlov and R. B. Panin, Izv. Akad. Nauk SSSR, Ser. Fiz. **47**, 889 (1983); in: Tezisy dokladov 32 Soveshchaniya po yadernoĭ spektroskopii i strukture atomnogo yadra (Abstracts of Papers at the 32nd Symposium on Nuclear Spectroscopy and Nuclear Structure), Nauka, Leningrad (1982), p. 240.
[11]A. Klein *et al.*, Phys. Rev. C **25**, 82 (1982).
[12]V. Paar, in: Interacting Bosons in Nuclear Physics (ed. F. Iachello), Plenum Press, New York (1979).
[13]G. Kyrchev, Nucl. Phys. **A349**, 416 (1980).
[14]R. V. Jolos, F. Dönau, and D. Janssen, Preprint R4-8077 [in Russian], JINR, Dubna (1974).
[15]A. Arima and F. Iachello, Phys. Rev. Lett. **35**, 1069 (1975); Ann. Phys. (N.Y.) **99**, 253 (1976).
[16]P. O. Lipas *et al.*, Phys. Scr. **27**, 8 (1983).
[17]A. Arima and F. Iachello, Ann. Phys. (N.Y.) **111**, 201 (1978).
[18]L. Wilets and M. Jean, Phys. Rev. **102**, 788 (1956).
[19]A. Arima and F. Iachello, Phys. Rev. Lett. **40**, 385 (1978); Ann. Phys. (N.Y.) **123**, 468 (1979).
[20]J. N. Ginocchio and M. W. Kirson, Phys. Rev. Lett. **44**, 1744 (1980); Nucl. Phys. **A350**, 31 (1980).
[21]M. W. Kirson, Ann. Phys. (N.Y.) **143**, 448 (1982).
[22]A. E. L. Dieperink *et al.*, Phys. Rev. Lett. **44**, 1747 (1980); A. E. L. Dieperink and O. Scholten, Nucl. Phys. **A346**, 625 (1980).
[23]M. Moshinsky, Nucl. Phys. **A338**, 156 (1980).
[24]A. Bohr and B. R. Mottelson, Phys. Scr. **22**, 468 (1980).
[25]P. Van Isaker and T. Q. Chen, Phys. Rev. C **4**, 684 (1981).
[26]D. H. Feng *et al.*, Phys. Rev. **23**, 1234 (1981).
[27]A. Weiguny, Z. Phys. A **301**, 335 (1981).
[28]A. Arima, T. Otsuka, F. Iachello, and I. Talmi, Phys. Lett. **66B**, 205 (1977).
[29]T. Otsuka *et al.*, Phys. Lett. **76B**, 139 (1978).
[30]T. Otsuka, A. Arima, and F. Iachello, Nucl. Phys. **A309**, 1 (1978); F. Iachello, in: Interacting Bosons in Nuclear Physics, Plenum Press, New York (1979), p. 3.
[31]A. E. L. Dieperink and K. Bijker, Phys. Lett. **116B**, 77 (1982).
[32]F. Iachello, Prog. Part. Nucl. Phys. **9**, 5 (1983).
[33]P. Van Isaker and G. Puddu, Nucl. Phys. **A348**, 1251 (1980).
[34]T. Tamura and T. Udagawa, Phys. Rev. Lett. **15**, 765 (1965).
[35]O. Scholten, in: Interacting Bosons in Nuclear Physics, Plenum Press, New York (1979), p. 59.
[36]P. D. Duval and B. R. Barrett, Phys. Rev. C **24**, 1272 (1981).
[37]R. V. Jolos *et al.*, Izv. Akad. Nauk SSSR, Ser. Fiz. **38**, 2059 (1975).
[38]M. Ogawa *et al.*, Phys. Rev. Lett. **41**, 289 (1978).
[39]R. F. Casten, Phys. Rev. Lett. **47**, 1433 (1981).
[40]R. L. Cill *et al.*, Phys. Lett. **118B**, 251 (1982).
[41]A. Wolf *et al.*, Phys. Lett. **123B**, 165 (1983).
[42]O. Scholten, Phys. Lett. **127B**, 144 (1983).
[43]A. Zemel, Phys. Lett. **126B**, 145 (1983).
[44]R. V. Jolos and D. Janssen, Yad. Fiz. **25**, 499 (1977) [Sov. J. Nucl. Phys. **25**, 268 (1977)].
[45]M. Sakai, Nucl. Phys. **104**, 301 (1967).
[46]I. A. Cizewski and R. F. Casten, Phys. Rev. Lett. **40**, 167 (1978).
[47]R. F. Casten, in: Interacting Bosons in Nuclear Physics, Plenum Press, New York (1979), p. 39.
[48]R. Büker *et al.*, Nucl. Phys. **A344**, 207 (1980).
[49]F. S. Stephens, Prog. Part. Nucl. Phys. **9**, 359 (1983).
[50]H. J. Weeks and T. Tamura, Phys. Rev. C **22**, 1323 (1980).
[51]U. Kaup and A. Gelberg, Z. Phys. A **293**, 311 (1979).
[52]H. J. Weeks *et al.*, Phys. Rev. C **24**, 703 (1981).
[53]K. Kumar, J. Phys. G **4**, 849 (1978).
[54]R. V. Jolos *et al.*, Yad. Fiz. **20**, 310 (1974) [Sov. J. Nucl. Phys. **20**, 165 (1975)].
[55]R. V. Jolos and D. Janssen, Conmunication E4-9358, JINR, Dubna (1976).
[56]D. N. Doĭnikov *et al.*, in: Tezisy dokladov 34 Soveshchaniya po yadernoĭ spektroskopii i strukture atomnogo yadra (Abstracts of Papers at the 34th Symposium on Nuclear Spectroscopy and Nuclear Structure), Nauka, Leningrad (1984), p. 68.
[57]K. I. Erokhina *et al.*, in: Tezisy dokladov 33 Soveshchaniya po yadernoĭ spektroskopii i strukture atomnogo yadra (Abstracts of Papers at the 33rd Symposium on Nuclear Spectroscopy and Nuclear Structure), Nauka, Leningrad (1983), p. 168.
[58]A. D. Efimov *et al.*, Preprint FTI-847 [in Russian], Leningrad (1983); Izv. Akad. Nauk SSSR, Ser. Fiz. **48**, 10 (1984).
[59]K. I. Erokhina *et al.*, in: Tezisy dokladov 33 Soveshchaniya po yadernoĭ spektroskopii i strukture atomnogo yadra (Abstracts of Papers at the 33rd Symposium on Nuclear Spectroscopy and Nuclear Structure), Nauka, Leningrad (1984), pp. 70–71.
[60]K. I. Erokhina *et al.*, Izv. Akad. Nauk SSSR, Ser. Fiz. **48**, 328 (1984); in: Tezisy dokladov 33 Soveshchaniya po yadernoĭ spektroskopii i strukture atomnogo yadra (Abstracts on Papers at the 33rd Symposium on Nuclear Spectroscopy and Nuclear Structure), Nauka, Leningrad (1984), p. 68.
[61]U. Kaup *et al.*, Z. Phys. A **310**, 129 (1983).
[62]T. Tatsuzaki and H. Taketani, Nucl. Phys. **A390**, 418 (1982).
[63]R. A. Meyer *et al.*, Phys. Rev. C **27**, 2217 (1983).
[64]P. D. Duval *et al.*, Phys. Lett. **124B**, 297 (1983).
[65]J. C. Well, Jr. *et al.*, Phys. Rev. C **22**, 1126 (1980).
[66]D. Bucurescu *et al.*, Nucl. Phys. **A401**, 22 (1983).
[67]G. F. Filippov *et al.*, Mikroskopicheskaya teoriya kollektivnykh vozbuzhdeniĭ atomnykh yader (Microscopic Theory of Collective Nuclear Excitations), Naukova Dumka, Kiev (1981).
[68]M. Vergnes, Inst. Phys. Conf. Ser. **49**, 25 (1980).
[69]J. H. Hamilton *et al.*, Phys. Rev. Lett. **47**, 1514 (1981).

[70]H. W. Fielding *et al.*, Nucl. Phys. **A281**, 389 (1977).
[71]J. Bron *et al.*, Nucl. Phys. **A318**, 335 (1979).
[72]P. D. Duval and B. R. Barrett, Phys. Lett. **100B**, 223 (1981).
[73]E. Nadjakov, Boson Models of Transitional Nuclei, Lectures at the Varna School on Nuclear Physics, Sofia (1981).
[74]M. Sambataro, Nucl. Phys. **A380**, 365 (1982).
[75]M. Sambataro and G. Molnár, Nucl. Phys. **A376**, 201 (1982).
[76]C. H. Druce *et al.*, J. Phys. G **8**, 1565 (1982).
[77]K. Heyde *et al.*, Phys. Lett. **132B**, 15 (1983).
[78]D. Schwalm, Nucl. Phys. **A396**, 339 (1983).
[79]P. Federman and S. Pittel, Phys. Rev. C **20**, 820 (1979).
[80]T. Otsuka, Nucl. Phys. **A368**, 244 (1981).
[81]T. Otsuka *et al.*, Phys. Rev. Lett. **48**, 378 (1982).
[82]D. R. Bes *et al.*, Phys. Rev. Lett. **48**, 1001 (1982).
[83]K. Sugavara-Tanabe and A. Arima, Phys. Lett. **110B**, 87 (1982).
[84]A. Bohr and B. R. Mottelson, Phys. Scr. **25**, 915 (1982).
[85]W. F. Davidson *et al.*, J. Phys. G **7**, 455, 843 (1981).
[86]D. E. Warner *et al.*, Phys. Rev. C **24**, 1713 (1981).
[87]A. Bohr and B. R. Mottelson, Phys. Scr. **25**, 28 (1982).
[88]D. D. Warner and R. F. Garten, Phys. Rev. Lett. **48**, 1385 (1982).

Translated by Julian B. Barbour